The RNA splicing factor Prp45 directs histone H2B ubiquitination through its C-terminal domain

Amit Paul, Ph.D.[1, 2] and Tracy Johnson, PhD [1, 2, 3]

[1]Department of Molecular Cell and Developmental Biology, University of California, Los Angeles, CA, USA, 90095
[2]Molecular Biology Institute, University of California, Los Angeles, CA, USA, 90095

[3]To whom correspondences should be addressed:

Tracy L. Johnson, UCLA Department of Molecular Cell and Developmental Biology, 610 Charles E Young Dr. S, Los Angeles, CA 90095
Tel (310) 206-2416; E-mail: tljohnson@ucla.edu

Summary

The protein Prp45 has well-characterized roles in RNA splicing. Although it has also been implicated in transcription elongation in metazoans, the mechanism for a role for Prp45 outside of splicing is unclear. Here, we combine genetic, proteomic, and biochemical approaches to show that the C-terminal region of the protein functionally and physically interacts with proteins involved in histone H2B ubiquitination, a mark of transcription elongation. Specifically, we find that Prp45 interacts with Lge1, the scaffold protein that is essential for the activity of the H2B ubiquitin ligase complex, through both Lge1's coiled-coil and intrinsically disordered domains, and these interactions are necessary to stabilize Lge1. In the absence of the Prp45 C-terminus interactions, the cells show a severe loss in H2B ubiquitination, a "Large" (Lge1) phenotype, and defective splicing of a subset of H2B-ubiquitination-dependent intron-containing transcripts. Together these data demonstrate an extra-spliceosomal role for the C-terminus of Prp45 in chromatin modification, RNA splicing, and proper cellular function.

Keywords: Prp45, Intrinsically Disordered Domain, chromatin modification, H2B ubiquitination, Lge1, Bre1, transcription elongation, RNA splicing

Introduction:

In the last several years, there has been a growing appreciation that the spliceosome assembles onto a pre-messenger RNA in a stepwise manner, co-transcriptionally, while the RNA is being synthesized by RNA polymerase II. A critical step in spliceosome assembly is the formation of the activated complex when the Prp19 complex (NTC) and NTC-associated factors (Prp45, Prp46, etc.) bind to the tri-snRNP complex. [1,2,3] The NTC plays a critical role in mediating spliceosome rearrangements necessary for catalysis. [2,4] The high-resolution Cryo-EM structure of the isolated activated complex shows that the N-terminal region of one of the NTC-associated factors, Prp45 appears to be buried inside the spliceosomal core, while the C-terminal region appears to protrude out of the structure.[5,6] This region of the structure might serve as a site for interaction with other splicing factors during stepwise assembly and conformational changes of the spliceosome or other proteins in the proximity of the spliceosome.

Prp45 is essential for the viability of the cell. Nonetheless, the cell can tolerate extensive truncation of Prp45 at its C-terminal end.[7] Prp45 containing only the first 169 out of the total 379 amino acids grows normally at 30°C, but growth is significantly impaired when the temperature is raised to 37°C.[8] Prp45 deleted of this C-terminal region (Prp45ΔCTR) shows reduced interaction with the second step helicase Prp22, thus affecting the fidelity of 3' splice site selection[9] and the splicing of those genes that do not have the optimal distance between the branchpoint site and 3' splice site or non-consensus 3' splice sites. Moreover, Prp45 deleted of this C-terminal region exhibits defects in the splicing of a subset of genes.[8]

We previously showed that co-transcriptional assembly of the spliceosome at the step of the Prp45 association is influenced by transcription elongation and the state of the chromatin. During transcription elongation, the Set2 histone methyl transferase methylates histone H3 at lysine 36 (H3K36me), a mark of active transcription.[10-12] H3K36 methylation is recognized by the chromodomain containing protein Eaf3[13,14,15] which, in turn, stabilizes the co-transcriptional association of Prp45 and the recruitment of the Prp19 complex, thus facilitating co-transcriptional splicing.[14]

As this example illustrates, there is strong evidence that histone modification affects RNA splicing, a relationship that is intuitive given the spatial and temporal proximity of the two reactions. However, the inverse relationship, that splicing factors affect chromatin modification, has also been described, particularly in metazoan cells.[16,17] However, direct mechanisms by which splicing factors affect chromatin modification have been difficult to determine. Prp45 is an intriguing candidate for a role in transcription and RNA splicing—potentially coordinating these reactions.

The homolog of Prp45, SKIP (Ski-interacting protein) in *Arabidopsis thaliana* and *Homo sapiens*, has been shown to have a role in transcription.[18,19] SKIP interacts with the Paf1 complex and activates the transcription of FLC to control flowering in Arabidopsis.[19,20] In humans SKIP associates with the Positive Transcription Elongation Factor b (pTEFb) to facilitate transcription elongation by HIV-1 Tat.[18] While a role in transcription has not been clearly shown in yeast, when the yeast protein Prp45 is fused with the DNA binding domain of SKIP, it can activate transcription.[7] Intriguingly, Prp45 shows genetic interactions with a number of chromatin-related enzymes, with strong interactions between Htz1 and the Swr complex members.[21]

The yeast genome architecture provides some hints about how introns may influence chromatin structure and modifications. Histone H2B is particularly interesting because H2B ubiquitination is enriched in highly expressed genes, particularly the ribosomal protein genes that contain introns.[22] Moreover, H2B ubiquitination marks the exon-intron boundary,[23,24] and the splicing of a subset of transcripts is particularly sensitive to H2B ubiquitination. These findings suggest that some aspects of the splicing machinery could contribute to the landscape of the histone modifications.

Bre1 is an E3 ligase that mono-ubiquitinates histone H2B at lysine 123 in the coding region during pol II elongation, in collaboration with the E2 conjugating enzyme Rad6.[25,26] A third protein Lge1, which was originally identified in a genetic screen for gene deletions that lead to a Large cell phenotype,[27] is essential for Bre1 catalytic activity.

Although Lge1 is largely unstructured and undergoes phase separation, the coiled-coil (CC) domain of Lge1, interacts with the N-terminal region of Bre1, and this interaction is necessary for Bre1-mediated H2BK123 ubiquitination in yeast.[28] Proper distribution of histone H2B mono-ubiquitination is necessary for gene activation and is regulated by cycles of deubiquitination. The de-ubiquitinase UBP8, which is part of the SAGA complex deubiquitinates H2B, particularly at the 5' prime region of the gene.[24] H2B mono-ubiquitination is an important mark modulating the global chromatin landscape and acts upstream of other important histone modifications associated with transcription elongation such as H3K4 methylation[25,29] and H3K36 methylation. [24,30]

Here we combine a genetics, proteomics, and biochemical approach to show that the C-terminal region of the Prp45 protein functionally and physically interacts with proteins involved in histone H2B ubiquitination. Consistent with these interactions, we find that the C-terminal region of Prp45 is required for efficient histone H2B mono-ubiquitination. To understand how Prp45 affects H2B ubiquitination, we analyze the Prp45 interactions with the ubiquitin ligase complex and find that Prp45 physically interacts with Lge1, and truncation of Prp45 leads to the destabilization of Lge1. This demonstrates that Ppr45 provides structural support for the Lge1 protein, especially at elevated temperatures. Consistent with a role for the C-terminal portion of Prp45 in Lge1 stability, truncation of Prp45 shows "large" cell morphology similar to *lge1*Δ that can be reversed by deletion of the deubiquitinase, indicating that the C-terminal domain of Prp45 has global effects on cellular morphology probably by affecting the H2B mono-ubiquitination level. Finally, we show that a subset of the effects that Prp45 has on splicing can be attributed to its role in H2B ubiquitination. These studies demonstrate a role for RNA splicing in chromatin modification, transcription elongation, and maintaining proper cell morphology and function.

Results

The C-terminal portion of Prp45 is required for optimal cell viability

Previous studies provided evidence that Prp45 is recruited co-transcriptionally and in close proximity to the chromatin. The Cryo-EM structure of yeast Bact spliceosome[5] visualized using Chimera-X suggests that the N-terminal end of the Prp45 protein has extensive interactions with spliceosomal proteins, but starting from 184 to 379 the C-terminal region appears to extend out of the spliceosome (Figure 1A). This C-terminal region encompasses the helical domain and the SH2-like domain which, in isolation, is predicted to be highly disordered (Figure 1B).

To begin to evaluate the function of the C-terminal region of the protein, we generated truncation mutants of Prp45—Prp45 (1-169), (1-174), (1-184), (1-260) and (1-296) based on the regions predicted by PONDR,[31] where the residues after 169, 174, 184, 260, and 296 were deleted, and the cells were grown at 30°C and 37°C (Figure 1C). The region including the SNW domain is essential for viability. Beyond the SNW domain, is the alpha helical domain that is well conserved from yeast to humans. The largest truncation, which eliminates this helical domain and a linker region between the SNW and the helical domain, Prp45(1-169) or Prp45ΔCTR, shows the most dramatic growth defect at elevated temperature. The strains with the second largest growth defects, Prp45(1-174) and Prp45(1-184), eliminate the helical domain. Prp45(1-260) and Prp45(1-296), containing the regions beyond the predicted disordered regions, grow like wild type cells at 37°C (Figure 1D).

The Prp45 C-terminus interacts with the H2B ubiquitination machinery

To identify specific proteins that interact with Prp45, specifically the C-terminal region, we performed proximity labeling. Briefly, biotin ligase BirA was added to the C-terminal region of either full length Prp45 or Prp45ΔCTR, and the strains were grown in the presence of

biotin. The biotinylated protein was immunoprecipitated using streptavidin beads, followed by mass spectrometry (Figure 2A). Full length Prp45 interacts with 251 different proteins (Supplementary Figure 1). Of these, 213 proteins show differential interactions when the C-terminal end is truncated. Six proteins show large changes (Supplementary Figure 1B). Not surprisingly, most of these are known splicing factors, such as Prp19 a fellow member of the NTC. The interactions between Prp45 and Brr2, Clf1, Prp46, and Spp2 are significantly reduced in Prp45ΔC, compared to the wild type. Interestingly, the level of Hsf1, which has extensive genetic interactions with several known splicing factors[32] also decreases significantly.

Thirty-eight proteins are not detected at all when the C-terminus is truncated, suggesting that they lose their interaction with Prp45 when the C-terminus is removed (Supplementary Figure 1A, Table 2). Hierarchical clustering of those 38 proteins reveals that, while many of the affected proteins are spliceosomal proteins, a second cluster includes proteins implicated in chromatin function. One of the interactions that is lost when the C-terminus of Prp45 is deleted is Bre1, the E3 ligase that, with its E2 Rad6, monoubiquitylates histone H2B.[33,34] Monoubiquitination of H2B requires a third component of this complex, Lge1, which interacts directly with Bre1 and is required for Bre1's H2B activity.[35,36]

To determine if there is a functional relationship between H2B ubiquitination and the Prp45 C-terminus, *BRE1*, *RAD6*, and *LGE1* were each deleted in combination with *prp45ΔCTR,* and the strains were grown at 30°C (data not shown) and 37°C. At 37°C, *prp45ΔCTR bre1Δ*, *prp45ΔCTR rad6Δ*, and *prp45ΔCTR lge1Δ* all show a severe growth defect compared to *prp45ΔCTR*, such that the *prp45ΔCTR bre1Δ* and *prp45ΔCTR lge1Δ* are inviable (Figure 2C). The synthetic genetic interactions between Ppr45 and Bre1/Rad6/Lge1 complex led us to assess whether the catalytic activity of the complex is at the core of this functional relationship. Previous studies have shown that Bre1 contains a RING domain at its C-terminal end, and tagging the Bre1 protein disrupts the RING domain and abrogates the catalytic activity of Bre1.[25] To abolish the catalytic activity, Bre1 was tagged with GFP at its C-terminal end in wild type cells and *prp45ΔCTR* strain.

Indeed, the catalytic activity is lost (Figure S2A), and similar to what is observed with *bre1*Δ*, prp45*Δ*CTR BRE1-GFP* cells are nonviable at 37°C (Supplementary Figure 2B). These results suggest that loss of H2B ubiquitination is responsible for the synthetic genetic interactions observed between Prp45 and Bre1 and its associated complex components. Since mutations that abrogate H2B ubiquitination show strong negative genetic interactions with Prp45, we predicted that mutations that stabilize ubiquitination would reverse the *prp45*ΔC growth defect. Ubp8 and Sgf73 are members of the SAGA complex and contribute to histone H2B deubiquitination.[37-40] Deletion of either *UBP8* or *SGF73* in the *prp45*Δ*CTR* strain rescues the 37°C growth defect (Figure 2C). Not surprisingly, deletion of the gene encoding the protein with the catalytic activity, *UBP8* shows the strongest suppression. To determine if suppression of the growth defect is specific to UBP8 mediated deubiquitination, we deleted UBP10, a deubiquitinase [24,41] in the *prp45*Δ*CTR. UBP10* deletion does not rescue the growth defect (Supplementary Figure 3). Indicating that the rescue phenotype is specific to UBP8 mediated deubiquitination of H2B.

Loss of the C-terminus of Prp45 leads to a decrease in H2B ubiquitination

In light of the functional and physical interactions between H2B ubiquitination machinery and Prp45, H2B ubiquitination was assessed in cells harboring a C-terminal truncation of Prp45. Analysis of the ubiquitome from wild type and *prp45*Δ*CTR* cells reveals a significant reduction in peak intensity of H2BK123 peptides in *prp45*Δ*CTR* (Figure 3B). This result was confirmed by western blot analysis; when wild type and *prp45*Δ*CTR* strains were grown at 30°C, there was a clear reduction in H2BK123ub in the prp*45*Δ*CTR* strain (Figure 3C), and the effect is even stronger at 37°C. In fact, there is a ~90% decrease in H2B ubiquitination in the *prp45*Δ*CTR* strain, although the levels of H2B remain the same (Figure 3D). Hence the C-terminal domain of Prp45 affects H2BK123 ubiquitination, and this is likely through modulating the catalytic activity of Bre1.

The C-terminal domain of Prp45 interacts with the ubiquitin ligase scaffold protein, Lge1

Although Bre1 is the ubiquitin-ligase responsible for H2B monoubiquitination, Bre1's activity is dependent on the Lge1 protein, especially when the cells experience replicative stress.[42] A recent analysis of the Lge1-Bre1 interaction reveals that Lge1 phase separates and forms condensates, which is mediated by its intrinsically disordered domain. The coiled-coil (CC) domain of Lge1 interacts with the N-terminal region of Bre1, and this interaction is necessary for Bre1 mediated H2BK123 ubiquitination.[28] Although Lge1-deleted cells normally can grow at 30°C and 37°C, the cells are morphologically larger compared to wild type cells.

While proximity labeling provides insights into the proximity of two interacting proteins, it is difficult to assess whether these interactions are direct or indirect since any protein residing within the 10nm diameter can be biotinylated.[43] In light of the observation of a Prp45 C-terminus-dependent interaction with Bre1, we looked for interactions between these proteins by co-immunoprecipitation but could not detect physical interaction between Bre1 and Prp45 (data not shown), suggesting that, perhaps, the interaction is indirect. We therefore considered proteins that are part of the H2B ubiquitination complex to determine if these interact with Prp45. Starting with Lge1, a cofactor of Bre1 that is required for its catalytic activity.[36] Full length Ppr45 immunoprecipitated Lge1; and the interaction is reduced when the C-terminus of Prp45 is truncated (Figure 4A). Based on the known structural information for Prp45 and Lge1, AlphaFold-multimer in Google colab-fold [44] was used to predict protein-protein interacting regions between the proteins. The results are depicted here using Chimera X (Figure 4B). Out of five interaction modules, four were found between the N-terminal region of Prp45 and the highly disordered domain of Lge1. The *in-silico* analyses also show interactions at the C-terminal region of Prp45 and the structured coiled-coil (CC) domain of the Lge1 protein (Figure 4B).

Although Lge1 is a highly disordered protein and most of its residues reside in the disordered region, as illustrated by the metaPredict (Figure 4C), it also contains the short, structured CC domain through which it interacts with the other proteins such as Bre1 [28]. To determine experimentally how the CC domain contributes to the Lge1-Prp45 interaction, co-immunoprecipitation was performed using Prp45 and Lge1 with a deletion of the CC domain, Lge1ΔCC. While Prp45 still can interact with the CC domain-deleted Lge1 protein, the signal is significantly decreased (Figure 4D). Hence, not only does Lge1 interact with Bre1 through its CC domain, but this domain also supports the Prp45 interaction.[28] Deletion of the CC domain leads to loss of H2B ubiquitination, comparable to a *BRE1* deletion (Figure 4E). When the CC domain of Lge1 is deleted in the *prp45ΔCTR* strain, and cells are grown at 37°C, these cells are nonviable, and the phenotype is comparable to the *prp45ΔCTR lge1Δ* strain (Figure 4F). These data suggest that the Prp45 effects on the catalytic activity of Bre1 are likely through its interactions with Lge1.

Prp45 interaction with Lge1 is required for Lge1 stability

In light of reports that Lge1 is a disordered protein and relatively unstable without Bre1, [36] we considered the possibility that Prp45 interaction with Lge1 is an important determinant of its stability. To determine if this is the case, western blot analysis was performed, and the blot was quantitated using image J. Although LGE1 RNA levels remain unchanged (Figure 5A, right), the Lge1 protein appears to be unstable in the *prp45ΔCTR* strain when compared to the Lge1 protein isolated from wild type cells, particularly at 37°C (Figure 5A, left). This suggests the C-terminal domain of Prp45 is required to maintain the stability of Lge1.

To further assess whether Prp45 contributes to Lge1 stability, Lge1 levels were analyzed in an auxin-inducible degron strain, where Prp45 is degraded in the presence of IAA over time (0, 15’, 30’, 60’). Indeed, Lge1 levels decrease in a time-dependent manner, along with Prp45. When cells are exposed to DMSO at the same time points, Lge1 protein levels are unchanged, indicating IAA (and hence Prp45) dependent loss of Lge1 (Figure 5B).

Hence, Prp45 is required to maintain the stability of Lge1. Consistent with this, H2BK123ub levels are gradually reduced with the degradation of Prp45 and the Lge1 protein (Figure 5B).

To determine if the Lge1 protein becomes unstable even at 30°C in the *prp45ΔCTR* strain, the Lge1 protein was tagged with a degron at its C-terminal end and a Kanamycin resistance marker was included at the N-terminal end under the native Lge1 promoter in wild type and *prp45ΔCTR* strain (Figure 5C, schematic). The cells were grown and serially diluted on a YPD + Kan + IAA plate (Figure 5C, growth assay). The results show a clear growth difference between Lge1 degron in the wild type background and Lge1 degron in the *prp45ΔCTR* strain on the selective plate. The degradation of Lge1 in the presence of IAA causes loss of kanamycin resistance and hence the growth is reduced, but the *prp45ΔCTR* amplifies the growth defect, consistent with enhanced Lge1 destabilization when the CTR of Prp45 is absent.

To determine whether the CC domain contributes to Prp45-dependent Lge1 protein stability, the CC domain of Lge1 protein was deleted when Prp45 is either full length or in a C-terminally truncated. At 30°C the effects on the Lge1ΔCC protein is modest. Lge1ΔCC protein levels decrease significantly at 37°C, even in the wild type strain, and is barely detected in the *prp45ΔCTR* strain. (Figure 5D).

While the interaction between the C-terminal region of Prp45 and Lge1 provides a clear mechanism for how Prp45 affects H2B-ubiquitination, the results led us to revisit the genetic interactions between Prp45 C-terminus and factors involved in H2B Ubiquitination. The genetics (Figures 2C and 4F) indicate strong functional interactions between Prp45 and the Histone H2B ubiquitination complex. However, if the only relationship between Prp45 and chromatin is mediated through this pathway, we might not predict synthetic lethality. For example, genetic depletion of Lge1, i.e. *LGE1* deletion, and destabilization of Lge1 through Prp45 truncation would be predicted to have a similar outcome, Prp45ΔC would not be expected to grow worse than *lge1Δ*, as we observe in the *lge1Δ prp45ΔC* strain. Similarly, destabilization of Lge1 through Prp45 truncation

leads to a dramatic decrease in H2B-ub, as does deletion of *BRE1*. If the only relationship between Prp45 and chromatin is mediated through effects on the H2B ubiquitination pathway, *prp45ΔC* would not be expected to grow worse than *bre1Δ*. Nonetheless, we observe a severe synthetic growth defect when *bre1Δ* and *prp45ΔC* are combined significantly worse than either mutation alone. In other words, when cells have a loss of H2B-ub, they become more dependent on a functional Prp45, leaving open the possibility that the Prp45 C-terminus may have other, chromatin-related function(s).

To this end, we predicted that gene deletions that lead to synthetic lethality with *bre1Δ* or *lge1Δ* (neither of which usually show a growth defect) would also be synthetically lethal with *prp45ΔCTR*. So, we surveyed the landscape of genetic interactions that are shared between *prp45ΔCTR* and *lge1Δ* or *bre1Δ*. Our own studies reveal significant overlaps. For example, *set2Δ* is synthetically lethal with *lge1Δ* and *bre1Δ*[45, 33, 32, 46] a phenotype shared with *prp45ΔCTR* (Supplemental Figure 4). Other gene deletions that lead to synthetically lethal when combined with *bre1Δ* and *lge1Δ* include htz1Δ, swr1Δ, swc3Δ, swc5Δ and Npl3.[33,47,46,48] These are also synthetically lethal when combined with *prp45ΔCTR* (Data not shown[21,22]). Taken together, these suggest that the role we show here for the Prp45 C-terminus-Lge1/Bre1 interaction is part of a network of chromatin-related functions that are essential for cell survival.

Loss of the Prp45-Lge1 mediated H2B ubiquitination leads to abnormal cell morphology and H2B-dependent splicing defects

Lge1 was first identified in a screen for genes whose deletion led to a disruption in size homeostasis. Although *LGE1* is not essential for cell viability, morphologically, the cells appear to have this large phenotype when this gene is deleted.[27] Previous studies have shown that *prp45ΔCTR* cells are large, elongated, and highly heterogeneous in nature.[9] Given these similarities, we performed a comparative study of the cell sizes of *prp45ΔCTR* and *lge1Δ* relative to WT cells. As previously reported, *prp45ΔCTR* strains were larger and slightly elongated compared to the wild type strain (Figure 6A);

*prp45*Δ*CTR* strains are almost 2.5 times larger than the WT cell and similar in size to lge1Δ (Figure 6A and graph). Since H2B ubiquitination is significantly decreased in the *prp45*Δ*CTR* strain and H2B ubiquitination has been shown to be involved in maintaining cell size,[49] we predicted that reversing the H2B ubiquitination defect, by deleting *UBP8*, might restore cell size. Not only does this mutation restore proper growth of the *prp45*Δ*CTR* strain (Figure 2C), but it also restores H2B ubiquitination (Figure 6B) and, importantly, *ubp8*Δ reverses the elongated cell phenotype and restores proper cell size (Figure 6C).

Finally, several groups have reported that histone H2B monoubiquitination affects the splicing of a small subset of intron-containing genes under normal growth conditions [22]. This result is intriguing in light of other studies that suggest that H2B ubiquitination marks exon-intron boundaries in budding yeast.[23] Our results raise the possibility that, although Prp45 is a Bonafide splicing factor, some of its effects on splicing may be specifically due to its role in H2B ubiquitination. To investigate the change in splicing upon the loss of the C-terminal end of Prp45, total RNA was isolated from WT, *prp45* Δ*CTR* strain, and specific RNAs were analyzed by RT-PCR. While the splicing of numerous introns is severely affected by deletion of the CTR, particularly at high temperature, reversing the H2B defect does not reverse the splicing defect (Figure 6D, left). Moreover, *BRE1* deletion also does not cause defective splicing, and deletion of *BRE1* in the *prp45*Δ*CTR* strain has the same splicing defect as *prp45*Δ*CTR*. These are examples seen for most intron-containing genes queried. On the other hand, when we analyze the splicing of other transcripts, e.g. *COF1* and *MAY24* in *Prp45*Δ*CTR* and *bre1*Δ deletion strains, we find that the un-spliced forms of the RNAs accumulate (Figure 6D, right), and the defect is reversed when *UBP8* is deleted in the *prp45*Δ*CTR* strain. These data suggest that some, but not all, of the Prp45-mediated role in splicing is through effects on H2B ubiquitination. Work is underway to determine the relative contribution of the different roles of the Prp45 C-terminus interactions, as suggested by both the physical and genetic analyses, in RNA splicing.

These data lead to a model whereby, the Prp45 C-terminus stabilizes a critical chromatin modifying protein to establish the state of the chromatin at intron-containing genes and the global effects of H2B ubiquitination in yeast cells.

Discussion:

Prp45 is a structurally conserved protein that is conserved from yeast to humans. While in *S. cerevisiae,* Prp45 has been characterized for its role in splicing, its homolog SNW1 and SKIP in *Arabidopsis thaliana* and mammals, respectively, have been shown to have role in flowering time initiation and transcriptional activation.[19,20] Here, we showed that Prp45 is also involved in extra-spliceosomal regulation of gene expression, particularly chromatin modification. Using genetics, proteomics, and biochemical approaches we identify a role for the C-terminal region of the splicing factor Ppr45 in H2B monoubiquitination.

As described above, much of the Prp45 protein is highly disordered with an extensive low complexity domain (LCD). LCDs facilitate the formation of biomolecular condensates [50,51], thus separating specific biochemical functions. The disordered nature of Prp45 is likely involved in biomolecular condensate formation during splicing, thus enriching splicing factors and other important proteins to facilitate efficient spliceosome assembly and splicing catalysis. This condensate formation also can facilitate the coordination of biochemical processes,[52,53,54] which is the role that Prp45 appears to play here.

Here we introduce a second highly disordered protein, Lge1, which interacts with Prp45. Approximately 85% of its amino acid residues are in disordered region (Figure 4C) forming LLPS. The disordered nature of Lge1 is critical for Bre1 recruitment to nucleosomes, and its H2B ubiquitination. We believe that these studies explain the observation that H2B is enriched at introns and help to define the exon-intron architecture [23]. Since Prp45 is a component of the splicing machinery, it is not surprising that proteins that interact with Prp45 would have a disproportionate effect on intron-containing genes. Intriguingly, not all ICG genes are similarly affected by the loss of histone H2B,[22] nor is

the splicing defect observed in *prp45ΔCTR* reversed by deleting the *de*ubiquitinase *UBP8,* even though this mutation restores H2B ubiquitination (Figure 6D). These data suggest that particular features of the intron determine sensitivity to H2B levels. We are working to define the internal "logic" of splicing's dependence or independence from H2B.

We are also considering the possibility that the presence of H2B at ICGs may affect some other aspect of these genes' expression besides splicing. Notably, H2B is enriched at some of the most highly expressed genes, such as the ribosomal protein genes. It is possible that deposition of H2B on these genes contributes to their high expression. In turn, high levels of intron-containing RNA increase the recruitment of splicing factors such as Prp45 to contribute to a stabilizing environment for Lge1. Thus, the interaction between Prp45 C-terminus and Lge1 may provide a positive feedback loop controlling the global levels of H2B as shown in Figures 3, 5B, and 6B.

Since H2B is essential for controlling cell size, it is not surprising, that a general feature that cell size is impacted with Prp45 is truncated (and Lge1 is rapidly depleted). The fact that this phenotype is reversed when *UBP8* is deleted, reinforces that it is Prp45's role in H2B ubiquitination that underlies its role in cell size homeostasis (Figure 6C). Why connect histone H2B deposition to a protein associated with intron-containing genes? Perhaps the load of highly expressed genes, such as ribosomes, the largest class of intron-containing genes, must be coordinated with cell division. When these processes are dysregulated, cell division is impaired.

Of course, we cannot rule out that Prp45 can interact with the chromatin or histone modifying enzymes outside of the spliceosome or that it associates with intron less genes independent of the rest of the spliceosome. In fact, we do observe some Prp45 signals when we carry out ChIP although the occupancy is considerably less than what is observed at intron-containing genes.

Finally, the genetic interactions we observe between Prp45ΔC and *bre1*Δ or *lge1*Δ mirror the interactions that the H2B ubiquitination machinery has with other chromatin modifying

machinery. The results hint at cross histone interactions that form an intricate network of gene expression. Prp45 C-terminus plays an important role in establishing the levels of one of these important marks.

Acknowledgements:

AP, TLJ, and work in the Johnson lab is supported by the NIH (R35GM149290).

Figure Legends

Figure 1. Prp45 has a disordered c-terminus that is required for viability at elevated temperature

A. Structure of Prp45 (shown in magenta). Cryo-EM structure of precatalytic spliceosome of *S cerevisiae* viewed using chimera X. **B**. Schematic of the domain architecture of the Prp45 protein. The disordered region of the protein is predicted by PONDR. **C.** Prp45 C-terminal truncated mutants were grown at 30°C and serially diluted on YPD and incubated at 30°C or 37°C (four days each).

Figure 2. The Prp45 C-terminus interacts with transcription elongation factors

A. Schematic of the *in vivo* biotinylation assay. **B.** Prp45's *in vivo* interaction partner identification by TurboID. Hierarchical clustering was performed using STRING for those proteins whose interaction was lost in the Prp45 C-terminal truncated strain. C. H2B-ub ligase complex deletions (*bre1*Δ, *rad6*Δ, *lge1*Δ) exacerbate Prp45ΔCTR growth defect; deletion of H2B deubiquitinase complex components (*ubp8*Δ and *sgf73*Δ) suppresses it. Cells are 10-fold serially diluted, plated on YPD, and grown at 37°C for four days.

Figure 3. C-terminal truncation of Prp45 abrogates histone H2BK123 ubiquitination.

A. Schematic of *in vivo* ubiquitin-labeling using WT or *prp45ΔCTR* cells **B.** Quantification of ubiquitylated H2BK123 peptides in WT and the *prp45ΔCTR* strain. **C.** Western blot analysis of ubiquitylated histone H2B from whole cell extracts isolated from WT and *prp45ΔCTR* strains grown at 30°C (anti-H2BK123-ub) **D.** Western blot analysis of ubiquitylated histone H2B of whole cell extracts isolated from WT and *prp45ΔCTR* strains grown at 37°C, an increasing amount of lysates were loaded on to the 15% SDS PAGE and ubiquitinated H2B or H2B were detected by anti-H2BK123ub or anti-H2B.

Figure 4. The C-terminus of Prp45 interacts with the coiled-coil domain of Lge1. A: Prp45-HA and Prp45ΔCTR-HA were immunoprecipitated with Anti-HA antibody and immunoblotted with Anti-FLAG antibody to detect Lge1. 2% input of total lysate was immunoprecipitated. Asterisk in lanes 2, 3, 5, and 6 indicates the heavy chains of the

antibody. **B.** *In silico* Prp45 and Lge1 interaction analysis by AlphaFold multimer and visualized in Chimera X. Prp45 protein labeled purple; the Lge1 protein is labeled gold. **C.** The disordered and structural domains of the Lge1 protein are mapped using Metapredict. The red line indicates the disordered region whereas, the blue line indicates the predicted structured domain. **D.** CC domain of Lge1 is required for its optimal binding with Prp45 protein: Prp45-HA was immunoprecipitated with Anti-HA antibody and immunoblotted with Anti-FLAG antibody to detect Lge1ΔCC. 2% input of total lysate was immunoprecipitated. **E.** Whole cell lysates isolated from WT, *lge1ΔCC,* and *bre1Δ* grown at 30°C and analyzed by western blot for detection of H2BK123 and H2B using anti-H2BK123 anti-H2B antibodies. **F.** WT, *prp45ΔCTR*, *prp45ΔCTR lge1Δ*, *prp45ΔCTR lge1ΔCC,* and *lge1ΔCC* cells were grown in YPD, 10-fold serially diluted on YPD and incubated at 30°C or 37°C for four days

Figure 5. The C-terminal structural domain of Lge1 is required for its stability. A. Western blot analysis of whole cell extracts from WT and *prp45ΔCTR* cells grown at 37°C Lge1-FLAG was detected using anti-FLAG antibody. Quantification is shown below each lane. The cDNA level of Lge1 was also checked at 37°C to show that there is no change in the Lge1 gene expression level between wild type and *prp45ΔCTR* strain (right image). **B.** Western blot analysis of Lge1 protein upon auxin-inducible degradation of Prp45 when cells are incubated IAA at different time points (0, 15', 30', and 60'). DMSO control is shown in lanes 1-4. Prp45-AID and Lge1 are detected using anti-HA and anti-FLAG antibodies, respectively. Ubiquitylated H2BK123 and H2B were detected using anti-H2BK123-ub and anti-H2B antibodies. **C.** Growth assay illustrating Lge1 instability unstable, at 30°C. Lge1 is N-terminally tagged with a Kanamycin resistance cassette and C-terminally tagged with degron sequence under the native Lge1 promoter in wild type and *prp45ΔCTR* strains. Cells are 10-fold serially diluted on a YPD + kanamycin +IAA plate and incubated at 30°C.

D. Western blot detection of Lge1ΔCC. Whole cell extract was isolated from *PRP45-Full Length (FL)* or *prp45ΔCTR*-HA. Strains were grown at 30°C and 37°C. H2B is provided as a loading control.

Figure 6. The Prp45 C-terminus, through its activity in H2B ubiquitination, is required for proper cell morphology and Prp45 function. A: (Left) Confocal imaging of WT, *prp45ΔCTR* and *lge1Δ*. Cells are grown to OD_{600} 0.6, washed with PBS, stained with 10ug/mL of DAPI, and washed again with PBS. **(Right)** P-values from unpaired one-way ANOVA with Tukey post hoc analysis; n=75. **B.** H2BK123 ubiquitination detected from WCE of WT, *prp45ΔCTR,* and *prp45ΔCTR ubp8Δ*. **C. (Left)** Confocal imaging of WT, *prp45ΔCTR,* and *prp45ΔCTR ubp8Δ* strains grown to OD600 0.6 at 37°C **(Right)** P-values from unpaired one-way ANOVA with Tukey post hoc analysis; n=75. **D. (Left)** RT-PCR analysis of splicing of HPC2, VSP75, NCB2 in WT, *prp45ΔCTR*, *bre1Δ*, *prp45ΔCTR bre1Δ*, *prp45ΔCTR ubp8Δ* and *ubp8Δ* strains. RT-PCR products are separated on a 1.7% agarose gel, with SCR1 being used as a loading control. **(Right)** RT-PCR analysis of splicing changes of COF1, MAY24 in WT, prp*45ΔCTR*, *bre1Δ*, *prp45ΔCTR bre1Δ*, *prp45ΔCTR ubp8Δ* and *ubp8Δ strain*. Products are separated on a 1.8% agarose gel. SCR1 is used as a loading control.

Figure 7. Model of Prp45 effects on histone H2B ubiquitination

Supplementary Figure 1. The total interactors of Prp45 identified by in vivo biotinylation. A: The Venn diagram indicates 38 unique interactors specific to the full length Prp45 only and 213 interactors that are common between full length and truncated Prp45 protein. B: Hierarchical clustering of the interactors that show significant change in interaction with Prp45 FL and Prp45ΔCTR. Prp19 shows significantly increased interaction with Prp45ΔCTR as compared to the full length Prp45, whereas BRR2, SPP2, PRP46, CLF1, PRP45, CBF1, TRM82, HSP12 show significant reduction in interaction when the C-terminal end of Prp45 is deleted.

Supplementary Figure 2. C-terminal tagging of Bre1 causes loss of its catalytic activity. A: Western blot analysis of ubiquitylated histone H2B and H2B from whole cell extracts isolated from WT, *BRE1 GFP*, *prp45ΔCTR Bre1 GFP* strains grown at 30°C (anti-H2BK123-ub and anti-H2B). B: WT, *BRE1 GFP,* and *prp45ΔCTR BRE1 GFP* cells were grown in YPD, 10-fold serially diluted on YPD, and incubated at 30°C or 37°C for four days

Supplementary Figure 3. UBP10 is not part of the deubiquitinase machinery rescuing the growth defect. WT, *prp45ΔCTR*, *prp45ΔCTR ubp10, and ubp10* cells were grown in YPD, 10-fold serially diluted on YPD, and incubated at 37°C for four days.

Supplementary Figure 4. Prp45 shows synthetic lethality with chromatin modifiers. A. Set2 was deleted in *prp45ΔCTR* strain and growth assay was done both at 30°C and 37°C. The *prp45ΔCTR set2Δ* strains show synthetic lethality at elevated temperature.

Materials and Methods

Strains and growth conditions:

All strains of *S. cerevisiae* used in this study are listed in Table S1. All strains are derived from BY4741. Prp45 degron strain was generated by integrating Adh1/AtTIR1 into the HIS3 locus. AID-HA-Hyg was added to the C-terminal of endogenous Prp45 by standard replacement by marker cassette.[62] Endogenous C-terminal tagged strains were generated by homologous recombination followed by PCR amplification from the pFA6a-3HA-kanMX6, and pFA6a-5FLAG-NatMX6 plasmids as described previously.[62] *Lge1*, *UBP8*, *UBP10*, and *Bre1* were knocked out by replacing the KanMX6 cassette. Cells were grown on YPD (1% yeast extract, 2% peptone, and 2% glucose) or synthetic drop out media at 30°C and 37°C.

Growth assay:

5mL overnight cultures were transferred to a fresh 50mL YPD and grown at 30°C until the OD reaches 0.5. Cells were 10-fold serially diluted and spotted on YPD or YPD + Kan + IAA plates. Plates were kept at 30°C and 37°C to observe the effect of elevated temperature.

In vivo depletion of Prp45 and Lge1:

Prp45-AID-HA and Lge1-AID-HA strains were grown on YPD at 30°C for 1hr followed by 1mM IAA (I5148, sigma) treatment for different time points. Cells were pelleted and kept at -80C.

Yeast nuclear extract preparation and western blotting:

Saturated overnight 5mL cultures were transferred to 50mL and allowed to grow at 30°C till they reached 0.8-1 OD. For elevated temperature stress cells were first grown at 30°C for 2hrs followed by transfer to 37°C and grown for 2 hrs. Cells were pelleted and resuspended in 500μL of lysis buffer (50mM HEPES pH7.5,150mMNaCl,1mMEDTA, 1% Triton X-100, 0.1% sodium deoxycholate) with protease inhibitor. An equal volume of 0.5 mm acid-washed glass beads (BioSpec) was added to the cell resuspension and the samples were lysed in a cell disruptor for 10 minutes at 4ºC. Proteins were separated in

an 8% SDS-PAGE for Lge1-FLAG, Prp45AID-HA and 15% SDS-PAGE for histone H2BK123 mono-ubiquitination and histone H2B. HA blots were probed with anti-HA antibody (clone 12CA5, Roche), FLAG blots were probed with anti-FLAG antibody (Sigma, catalog no F1804), histone H2BK123Ub1 blots were probed with anti-H2BK123Ub1(anti-ubiquity H2B,5546S; CST, Cell Signaling Technology, Danvers, MA, USA), and histone H2B blots were probed with anti-H2B (Active motif, catalog no 39210).

RNA isolation and RT-PCR analysis:

Yeast cells were grown until the A_{600} = 1.0. Total RNA was isolated using the hot acid phenol method. Yeast cells were treated with acidic phenol (P4682; Sigma) at 65 °C, and the RNA was extracted with phenol/chloroform/isoamyl alcohol with SDS followed by ethanol precipitation. Following total RNA isolation, 25μg of RNA was treated with DNaseI (Roche). 3ug of DNaseI-treated RNA was used for cDNA synthesis. The first strand of cDNA was generated using Maxima Reverse Transcriptase (ThermoFisher Scientific). Gene-specific primers are listed in Table S1. 1–2 μL of cDNA was used as the template in a 25μL PCR reaction. Primers that flank the intron were used to observe splicing changes. The PCR products were run on a 1.8% agarose gel (ethidium bromide added). Gels were then imaged on Image Lab (Bio-Rad).

Co-immunoprecipitation:

25mL overnight saturated culture was transferred to 125mL of fresh YPD and cells were grown until A_{600}=0.8-1. Cells were then pelleted and resuspended in 1 mL of lysis buffer with protease inhibitors. Acid-washed beads were added to the resuspension and samples were lysed in a cell disruptor for 10 minutes at 4ºC. The lysates were centrifuged at 13,000 rpm at 4ºC for 15 minutes to remove any insoluble material.

1 mL of lysate was precleared with 50 μL of Protein A/G agarose beads (sc-2003, Santa Cruz Biotechnology). 25 μL of precleared lysate was removed as input. 4 ug of anti-HA antibody (clone: 12CA5, Roche) was added to the 700 μL of clarified lysate and rotated at 4C overnight. Samples were incubated with 50uL of Protein A/G agarose beads for two

hours at 4C. Beads were then washed five times with lysis buffer and eluted by boiling with 2X SDS PAGE loading buffer.

Proximity labeling biotinylation and Mass-spectrometry:

5mL TurboID tagged overnight cultures were transferred to fresh 50mL YPD supplemented with 50uM biotin. Cells grew at 30°C until the OD of the cultures reached 0.8. cell pellets were resuspended in 250uL of RIPA buffer (50 mM Tris-HCl pH 7.5, 150 mM NaCl, 1.5 mM $MgCl_2$, 1 mM EGTA, 0.1% SDS, 1% NP-40, supplemented with 0.4% sodium deoxycholate, 1 mM DTT, 1 mM PMSF and 1x complete). Acid-washed beads were added to the resuspension and samples were lysed in a cell disruptor for 10 minutes at 4°C. The lysates were centrifuged at 13,000 rpm at 4°C for 15 minutes to remove any insoluble material. Lysates were briefly sonicated and treated with benzonase (Medchem exp) for 2 hours at 4°C to digest DNA and RNA. 10mg of total proteins were subjected to affinity purification using 50uL streptavidin (GE) at 4°C for 3hrs. Beads were then washed once with wash buffer (50 mM Tris-HCl pH 7.5, 2% SDS) followed three time wash with RIPA buffer containing DTT (50 mM Tris-HCl pH 7.5, 150 mM NaCl, 1.5 mM $MgCl_2$, 1 mM EGTA, 0.1% SDS, 1% NP-40, 1 mM DTT). Finally, the beads were washed five times with 20 mM ammonium bicarbonate. All the washes were done for 5 minutes at room temperature in a nutator. For mass-spectrometric analysis, streptavidin bound proteins were reduced in 10mM DTT followed by alkylation with 15mM iodoacetamide.

Protein-bound beads were subjected to trypsin digestion at 37°C overnight and stopped by the addition of formic acid (final concentration of 1%). Peptides were then extracted using acetonitrile, lyophilized, and resuspended in 0.1% trifluoroacetic acid (TFA) to desalt on ZipTips. (EMD Millipore) cleanup of peptide samples was performed as described previously.[63] Trypsin digested samples were analyzed by LC/MS. MaxQuant software package version 1.5.1.2 was used to analyze the data using the S cerevisiae Uniprot proteome. Peak intensity of peptides was used for relative quantification of proteins.

***In silico* protein interaction analysis:**

Alphafold2 was used to generate three-dimensional protein structures and Google Colabfold was used to analyze the protein interaction. The best fit model was fetched to ChimeraX 1.9 and subsequent analysis was done in ChimeraX 1.9 including probable contact sites between the interacting proteins.

Microscopy and image quantification:

Wild type and mutant strains were stained with DAPI and observed under the 63X oil immersion lens. The images were quantified using image J.

Statistical analysis:

One way ANOVA with Tukey post-hoc analysis was used to determine the P-values.

Supplementary Material

Genotype	Source
MATa his3Δ1 leu2Δ0 met15Δ0 ura3Δ0 (WT)	Open Biosystems
MATa PRP45-HA::KANMX6 his3Δ1 leu2Δ0 met15Δ0 ura3Δ0	This study
MATa PRP45ΔCTR-HA::KANMX6 his3Δ1 leu2Δ0 met15Δ0 ura3Δ0	This study
MATa PRP45-HA::KANMX6 Lge1-FLAG::NATMX6 his3Δ1 leu2Δ0 met15Δ0 ura3Δ0	This study
MATa PRP45ΔCTR-HA::KANMX6 Lge1-FLAG::NATMX6 his3Δ1 leu2Δ0 met15Δ0 ura3Δ0	This study
MATa PRP45-HA::KANMX6 Lge1ΔCC-FLAG::NATMX6 his3Δ1 leu2Δ0 met15Δ0 ura3Δ0	This study
MATa PRP45(1-174)-HA::KANMX6 his3Δ1 leu2Δ0 met15Δ0 ura3Δ0	This study
MATa PRP45(1-184)-HA::KANMX6 his3Δ1 leu2Δ0 met15Δ0 ura3Δ0	This study
MATa PRP45(1-260)-HA::KANMX6 his3Δ1 leu2Δ0 met15Δ0 ura3Δ0	This study
MATa PRP45(1-296)-HA::KANMX6 his3Δ1 leu2Δ0 met15Δ0 ura3Δ0	This study
MATa Bre1-GFP::KANMX6 his3Δ1 leu2Δ0 met15Δ0 ura3Δ0	This study
MATa Bre1-GFP::KANMX6 PRP45ΔCTR-FLAG::NATMX6 his3Δ1 leu2Δ0 met15Δ0 ura3Δ0	This study
MATa UBP8Δ-FLAG::NATMX6 his3Δ1 leu2Δ0 met15Δ0 ura3Δ0	Open Biosystems
MATa UBP8Δ-FLAG::NATMX6 PRP45ΔCTR-HA::KANMX6 his3Δ1 leu2Δ0 met15Δ0 ura3Δ0	This study
MATa UBP10Δ-FLAG::NATMX6 PRP45ΔCTR-HA::KANMX6 his3Δ1 leu2Δ0 met15Δ0 ura3Δ0	This study

MATa LGE1Δ-FLAG::NATMX6 PRP45ΔCTR-HA::KANMX6 his3Δ1 leu2Δ0 met15Δ0 ura3Δ0	This study
MATa LGE1ΔCC-FLAG::NATMX6 PRP45-HA::KANMX6 his3Δ1 leu2Δ0 met15Δ0 ura3Δ0	This study
MATa LGE1ΔCC-FLAG::NATMX6 PRP45ΔCTR-HA::KANMX6 his3Δ1 leu2Δ0 met15Δ0 ura3Δ0	This study
MATa LGE1Δ-FLAG::NATMX6 his3Δ1 leu2Δ0 met15Δ0 ura3Δ0	Open Biosystems
MATa BRE1Δ-FLAG::NATMX6 his3Δ1 leu2Δ0 met15Δ0 ura3Δ0	Open Biosystems
MATa BRE1Δ-FLAG::NATMX6 PRP45ΔCTR-HA::KANMX6 his3Δ1 leu2Δ0 met15Δ0 ura3Δ0	This study
MATa RAD6Δ-FLAG::NATMX6 his3Δ1 leu2Δ0 met15Δ0 ura3Δ0	Open Biosystems
MATa RAD6Δ-FLAG::NATMX6 PRP45ΔCTR-HA::KANMX6 his3Δ1 leu2Δ0 met15Δ0 ura3Δ0	This study
MATa PRP45-AID-HA::Hyg LGE1-FLAG:NATMX6 his3Δ1 leu2Δ0 met15Δ0 ura3Δ0	This study
MATa SGF73Δ-FLAG::NATMX6 PRP45ΔCTR-HA::KANMX6 his3Δ1 leu2Δ0 met15Δ0 ura3Δ0	This study
MATa SGF73Δ-FLAG::NATMX6 his3Δ1 leu2Δ0 met15Δ0 ura3Δ0	Open Biosystems

Primer name	Sequence (5' to 3')	Purpose
COF1 F	AGA CTG GTT AGC AAC TAC G	RT-PCR
COF1R	TCG TAA GAT GGG TCA GTA GAG	RT-PCR
VPS75 F	ACA CTG CCA ATG ATG AGT G	RT-PCR
VPS75 R	TCC AGA ACT CTG CAA TTT CG	RT-PCR
HPC2 F	CCTCCACGA CCATATTCAA ACGATTGG	RT-PCR
HPC2 R	GGAACCAGAAATTATAATGGGAGACGG	RT-PCR

SCR1 F	AAGGGATAGTTCTCTATTCCGCACC	RT-PCR
SCR1 R	CACAATGTGCGAGTAAATCCTGATG	RT-PCR

References Cited

1. Cheng, S.C., and Abelson, J. (1987). Spliceosome assembly in yeast. Genes Dev *1*, 1014-1027. 10.1101/gad.1.9.1014.
2. Chan, S.-P., Kao, D.-I., Tsai, W.-Y., and Cheng, S.-C. (2003). The Prp19p-associated complex in spliceosome activation. Science *302*, 279-282.
3. Albers, M., Diment, A., Muraru, M., Russell, C.S., and Beggs, J.D. (2003). Identification and characterization of Prp45p and Prp46p, essential pre-mRNA splicing factors. RNA *9*, 138-150. 10.1261/rna.2119903.
4. Chanarat, S., and Sträßer, K. (2013). Splicing and beyond: The many faces of the Prp19 complex. Biochimica et Biophysica Acta (BBA) - Molecular Cell Research *1833*, 2126-2134. https://doi.org/10.1016/j.bbamcr.2013.05.023.
5. Yan, C., Wan, R., Bai, R., Huang, G., and Shi, Y. (2016). Structure of a yeast activated spliceosome at 3.5 Å resolution. Science *353*, 904-911. 10.1126/science.aag0291.
6. Wan, R., Yan, C., Bai, R., Huang, G., and Shi, Y. (2016). Structure of a yeast catalytic step I spliceosome at 3.4 Å resolution. Science *353*, 895-904. 10.1126/science.aag2235.
7. Martinkova, K., Lebduska, P., Skruzny, M., Folk, P., and Puta, F. (2002). Functional Mapping of Saccharomyces cerevisiae Prp45 Identifies the SNW Domain as Essential for Viability. Journal of biochemistry *132*, 557-563. 10.1093/oxfordjournals.jbchem.a003257.
8. Hálová, M., Gahura, O., Převorovský, M., Cit, Z., Novotný, M., Valentová, A., Abrhámová, K., Půta, F., and Folk, P. (2017). Nineteen complex-related factor Prp45 is required for the early stages of cotranscriptional spliceosome assembly. Rna *23*, 1512-1524. 10.1261/rna.061986.117.
9. Gahura, O., Abrhámová, K., Skružný, M., Valentová, A., Munzarová, V., Folk, P., and Půta, F. (2009). Prp45 affects Prp22 partition in spliceosomal complexes and splicing efficiency of non-consensus substrates. Journal of Cellular Biochemistry *106*, 139-151. https://doi.org/10.1002/jcb.21989.
10. Venkatesh, S., and Workman, J.L. (2013). Set2 mediated H3 lysine 36 methylation: regulation of transcription elongation and implications in organismal development. Wiley Interdiscip Rev Dev Biol *2*, 685-700. 10.1002/wdev.109.
11. DiFiore, J.V., Ptacek, T.S., Wang, Y., Li, B., Simon, J.M., and Strahl, B.D. (2020). Unique and Shared Roles for Histone H3K36 Methylation States in Transcription Regulation Functions. Cell Reports *31*. 10.1016/j.celrep.2020.107751.
12. Mei, Y.-C., Feng, J., He, F., Li, Y.-M., Liu, Y., Li, F., Chen, Y., and Du, H.-N. (2021). Set2-mediated H3K36 methylation states redundantly repress the production of antisense transcripts: role in transcription regulation. FEBS Open Bio *11*, 2225-2235. https://doi.org/10.1002/2211-5463.13226.
13. Xu, C., Cui, G., Botuyan, M.V., and Mer, G. (2008). Structural basis for the recognition of methylated histone H3K36 by the Eaf3 subunit of histone deacetylase complex Rpd3S. Structure *16*, 1740-1750. 10.1016/j.str.2008.08.008.
14. Leung, C.S., Douglass, S.M., Morselli, M., Obusan, M.B., Pavlyukov, M.S., Pellegrini, M., and Johnson, T.L. (2019). H3K36 Methylation and the

Chromodomain Protein Eaf3 Are Required for Proper Cotranscriptional Spliceosome Assembly. Cell Reports *27*, 3760-3769.e3764. 10.1016/j.celrep.2019.05.100.
15. Guan, H., Wang, P., Zhang, P., Ruan, C., Ou, Y., Peng, B., Zheng, X., Lei, J., Li, B., Yan, C., and Li, H. (2023). Diverse modes of H3K36me3-guided nucleosomal deacetylation by Rpd3S. Nature *620*, 669-675. 10.1038/s41586-023-06349-1.
16. Kim, S., Kim, H., Fong, N., Erickson, B., and Bentley, D.L. (2011). Pre-mRNA splicing is a determinant of histone H3K36 methylation. Proceedings of the National Academy of Sciences *108*, 13564-13569. doi:10.1073/pnas.1109475108.
17. de Almeida, S.F., Grosso, A.R., Koch, F., Fenouil, R., Carvalho, S., Andrade, J., Levezinho, H., Gut, M., Eick, D., Gut, I., et al. (2011). Splicing enhances recruitment of methyltransferase HYPB/Setd2 and methylation of histone H3 Lys36. Nature Structural & Molecular Biology *18*, 977-983. 10.1038/nsmb.2123.
18. Brès, V., Gomes, N., Pickle, L., and Jones, K.A. (2005). A human splicing factor, SKIP, associates with P-TEFb and enhances transcription elongation by HIV-1 Tat. Genes Dev *19*, 1211-1226. 10.1101/gad.1291705.
19. Cao, Y., and Ma, L. (2019). To Splice or to Transcribe: SKIP-Mediated Environmental Fitness and Development in Plants. Front Plant Sci *10*, 1222. 10.3389/fpls.2019.01222.
20. Li, Y., Xia, C., Feng, J., Yang, D., Wu, F., Cao, Y., Li, L., and Ma, L. (2016). The SNW Domain of SKIP Is Required for Its Integration into the Spliceosome and Its Interaction with the Paf1 Complex in Arabidopsis. Molecular Plant *9*, 1040-1050. https://doi.org/10.1016/j.molp.2016.04.011.
21. Abrhámová, K., Groušlová, M., Valentová, A., Hao, X., Liu, B., Převorovský, M., Gahura, O., Půta, F., Sunnerhagen, P., and Folk, P. (2024). Truncating the spliceosomal 'rope protein' Prp45 results in Htz1 dependent phenotypes. RNA Biol *21*, 1-17. 10.1080/15476286.2024.2348896.
22. Hérissant, L., Moehle, E.A., Bertaccini, D., Van Dorsselaer, A., Schaeffer-Reiss, C., Guthrie, C., and Dargemont, C. (2014). H2B ubiquitylation modulates spliceosome assembly and function in budding yeast. Biol Cell *106*, 126-138. 10.1111/boc.201400003.
23. Shieh, G.S., Pan, C.H., Wu, J.H., Sun, Y.J., Wang, C.C., Hsiao, W.C., Lin, C.Y., Tung, L., Chang, T.H., Fleming, A.B., et al. (2011). H2B ubiquitylation is part of chromatin architecture that marks exon-intron structure in budding yeast. BMC Genomics *12*, 627. 10.1186/1471-2164-12-627.
24. Schulze, J.M., Hentrich, T., Nakanishi, S., Gupta, A., Emberly, E., Shilatifard, A., and Kobor, M.S. (2011). Splitting the task: Ubp8 and Ubp10 deubiquitinate different cellular pools of H2BK123. Genes Dev *25*, 2242-2247. 10.1101/gad.177220.111.
25. Wood, A., Krogan, N.J., Dover, J., Schneider, J., Heidt, J., Boateng, M.A., Dean, K., Golshani, A., Zhang, Y., Greenblatt, J.F., et al. (2003). Bre1, an E3 Ubiquitin Ligase Required for Recruitment and Substrate Selection of Rad6 at a Promoter. Molecular Cell *11*, 267-274. 10.1016/S1097-2765(02)00802-X.
26. Deng, Z., Ai, H., Sun, M., Tong, Z., Du, Y., Qu, Q., Zhang, L., Xu, Z., Tao, S., Shi, Q., et al. (2023). Mechanistic insights into nucleosomal H2B

monoubiquitylation mediated by yeast Bre1-Rad6 and its human homolog RNF20/RNF40-hRAD6A. Mol Cell *83*, 3080-3094.e3014. 10.1016/j.molcel.2023.08.001.

27. Jorgensen, P., Nishikawa, J.L., Breitkreutz, B.-J., and Tyers, M. (2002). Systematic Identification of Pathways That Couple Cell Growth and Division in Yeast. Science *297*, 395-400. doi:10.1126/science.1070850.
28. Gallego, L.D., Schneider, M., Mittal, C., Romanauska, A., Gudino Carrillo, R.M., Schubert, T., Pugh, B.F., and Köhler, A. (2020). Phase separation directs ubiquitination of gene-body nucleosomes. Nature *579*, 592-597. 10.1038/s41586-020-2097-z.
29. Vlaming, H., Molenaar, T.M., van Welsem, T., Poramba-Liyanage, D.W., Smith, D.E., Velds, A., Hoekman, L., Korthout, T., Hendriks, S., Altelaar, A.F.M., and van Leeuwen, F. (2016). Direct screening for chromatin status on DNA barcodes in yeast delineates the regulome of H3K79 methylation by Dot1. eLife *5*, e18919. 10.7554/eLife.18919.
30. Bilokapic, S., and Halic, M. (2019). Nucleosome and ubiquitin position Set2 to methylate H3K36. Nat Commun *10*, 3795. 10.1038/s41467-019-11726-4.
31. Kurgan, L., Hu, G., Wang, K., Ghadermarzi, S., Zhao, B., Malhis, N., Erdős, G., Gsponer, J., Uversky, V.N., and Dosztányi, Z. (2023). Tutorial: a guide for the selection of fast and accurate computational tools for the prediction of intrinsic disorder in proteins. Nature Protocols *18*, 3157-3172. 10.1038/s41596-023-00876-x.
32. Costanzo, M., VanderSluis, B., Koch, E.N., Baryshnikova, A., Pons, C., Tan, G., Wang, W., Usaj, M., Hanchard, J., Lee, S.D., et al. (2016). A global genetic interaction network maps a wiring diagram of cellular function. Science *353*. 10.1126/science.aaf1420.
33. Xiao, T., Kao, C.F., Krogan, N.J., Sun, Z.W., Greenblatt, J.F., Osley, M.A., and Strahl, B.D. (2005). Histone H2B ubiquitylation is associated with elongating RNA polymerase II. Mol Cell Biol *25*, 637-651. 10.1128/mcb.25.2.637-651.2005.
34. Zhao, F., Hicks, C.W., and Wolberger, C. (2023). Mechanism of histone H2B monoubiquitination by Bre1. Nature Structural & Molecular Biology *30*, 1623-1627. 10.1038/s41594-023-01137-x.
35. Song, Y.-H., and Ahn, S.H. (2010). A Bre1-associated Protein, Large 1 (Lge1), Promotes H2B Ubiquitylation during the Early Stages of Transcription Elongation*. Journal of Biological Chemistry *285*, 2361-2367. https://doi.org/10.1074/jbc.M109.039255.
36. Jueun Kim, Y.-K.A., Shinae Park, Jung-Shin Lee (2018). Bre1 mediates the ubiquitination of histone H2B by regulating Lge1 stability. FEBS letters.
37. Daniel, J.A., Torok, M.S., Sun, Z.-W., Schieltz, D., Allis, C.D., Yates, J.R., and Grant, P.A. (2004). Deubiquitination of Histone H2B by a Yeast Acetyltransferase Complex Regulates Transcription*. Journal of Biological Chemistry *279*, 1867-1871. https://doi.org/10.1074/jbc.C300494200.
38. Samara, N.L., Datta, A.B., Berndsen, C.E., Zhang, X., Yao, T., Cohen, R.E., and Wolberger, C. (2010). Structural Insights into the Assembly and Function of the SAGA Deubiquitinating Module. Science *328*, 1025-1029. doi:10.1126/science.1190049.

39. Köhler, A., Zimmerman, E., Schneider, M., Hurt, E., and Zheng, N. (2010). Structural basis for assembly and activation of the heterotetrameric SAGA histone H2B deubiquitinase module. Cell *141*, 606-617. 10.1016/j.cell.2010.04.026.
40. McCormick, M.A., Mason, A.G., Guyenet, S.J., Dang, W., Garza, R.M., Ting, M.K., Moller, R.M., Berger, S.L., Kaeberlein, M., Pillus, L., et al. (2014). The SAGA histone deubiquitinase module controls yeast replicative lifespan via Sir2 interaction. Cell Rep *8*, 477-486. 10.1016/j.celrep.2014.06.037.
41. Nune, M., Morgan, M.T., Connell, Z., McCullough, L., Jbara, M., Sun, H., Brik, A., Formosa, T., and Wolberger, C. (2019). FACT and Ubp10 collaborate to modulate H2B deubiquitination and nucleosome dynamics. Elife *8*. 10.7554/eLife.40988.
42. van der Horst, S.C., Kollenstart, L., Batté, A., Keizer, S., Vreeken, K., Pandey, P., Chabes, A., and van Attikum, H. (2025). Replication-IDentifier links epigenetic and metabolic pathways to the replication stress response. Nature Communications *16*, 1416. 10.1038/s41467-025-56561-y.
43. Larochelle, M., Bergeron, D., Arcand, B., and Bachand, F. (2019). Proximity-dependent biotinylation mediated by TurboID to identify protein-protein interaction networks in yeast. J Cell Sci *132*. 10.1242/jcs.232249.
44. Mirdita, M., Schütze, K., Moriwaki, Y., Heo, L., Ovchinnikov, S., and Steinegger, M. (2022). ColabFold: making protein folding accessible to all. Nature Methods *19*, 679-682. 10.1038/s41592-022-01488-1.
45. Krogan, N.J., Kim, M., Tong, A., Golshani, A., Cagney, G., Canadien, V., Richards, D.P., Beattie, B.K., Emili, A., Boone, C., et al. (2003). Methylation of histone H3 by Set2 in Saccharomyces cerevisiae is linked to transcriptional elongation by RNA polymerase II. Mol Cell Biol *23*, 4207-4218. 10.1128/mcb.23.12.4207-4218.2003.
46. Tong, A.H., Lesage, G., Bader, G.D., Ding, H., Xu, H., Xin, X., Young, J., Berriz, G.F., Brost, R.L., Chang, M., et al. (2004). Global mapping of the yeast genetic interaction network. Science *303*, 808-813. 10.1126/science.1091317.
47. Krogan, N.J., Baetz, K., Keogh, M.C., Datta, N., Sawa, C., Kwok, T.C., Thompson, N.J., Davey, M.G., Pootoolal, J., Hughes, T.R., et al. (2004). Regulation of chromosome stability by the histone H2A variant Htz1, the Swr1 chromatin remodeling complex, and the histone acetyltransferase NuA4. Proc Natl Acad Sci U S A *101*, 13513-13518. 10.1073/pnas.0405753101.
48. Venkatasubrahmanyam, S., Hwang, W.W., Meneghini, M.D., Tong, A.H., and Madhani, H.D. (2007). Genome-wide, as opposed to local, antisilencing is mediated redundantly by the euchromatic factors Set1 and H2A.Z. Proc Natl Acad Sci U S A *104*, 16609-16614. 10.1073/pnas.0700914104.
49. Hwang, W.W., Venkatasubrahmanyam, S., Ianculescu, A.G., Tong, A., Boone, C., and Madhani, H.D. (2003). A Conserved RING Finger Protein Required for Histone H2B Monoubiquitination and Cell Size Control. Molecular Cell *11*, 261-266. https://doi.org/10.1016/S1097-2765(02)00826-2.
50. Farag, M., Cohen, S.R., Borcherds, W.M., Bremer, A., Mittag, T., and Pappu, R.V. (2022). Condensates formed by prion-like low-complexity domains have

small-world network structures and interfaces defined by expanded conformations. Nature Communications *13*, 7722. 10.1038/s41467-022-35370-7.
51. Villegas, J.A., Heidenreich, M., and Levy, E.D. (2022). Molecular and environmental determinants of biomolecular condensate formation. Nature Chemical Biology *18*, 1319-1329. 10.1038/s41589-022-01175-4.
52. Pei, G., Lyons, H., Li, P., and Sabari, B.R. (2025). Transcription regulation by biomolecular condensates. Nature Reviews Molecular Cell Biology *26*, 213-236. 10.1038/s41580-024-00789-x.
53. Wang, Y., Li, S., Mokbel, M., May, A.I., Liang, Z., Zeng, Y., Wang, W., Zhang, H., Yu, F., Sporbeck, K., et al. (2024). Biomolecular condensates mediate bending and scission of endosome membranes. Nature *634*, 1204-1210. 10.1038/s41586-024-07990-0.
54. Dai, Y., Zhou, Z., Yu, W., Ma, Y., Kim, K., Rivera, N., Mohammed, J., Lantelme, E., Hsu-Kim, H., Chilkoti, A., and You, L. (2024). Biomolecular condensates regulate cellular electrochemical equilibria. Cell *187*, 5951-5966.e5918. 10.1016/j.cell.2024.08.018.
55. Shukla, P.K., Bissell, J.E., Kumar, S., Pokhrel, S., Palani, S., Radmall, K.S., Obidi, O., Parnell, T.J., Brasch, J., Shrieve, D.C., and Chandrasekharan, M.B. (2023). Structure and functional determinants of Rad6-Bre1 subunits in the histone H2B ubiquitin-conjugating complex. Nucleic Acids Res *51*, 2117-2136. 10.1093/nar/gkad012.
56. Shi, M., Zhao, J., Zhang, S., Huang, W., Li, M., Bai, X., Zhang, W., Zhang, K., Chen, X., and Xiang, S. (2023). Structural basis for the Rad6 activation by the Bre1 N-terminal domain. eLife *12*, e84157. 10.7554/eLife.84157.
57. Li, Y.M., Mei, Y.C., Liu, A.H., Wang, R.X., Chen, R., and Du, H.N. (2023). Gcn5- and Bre1-mediated Set2 degradation promotes chronological aging of Saccharomyces cerevisiae. Cell Rep *42*, 113186. 10.1016/j.celrep.2023.113186.
58. El-Saafin, F., Devys, D., Johnsen, S.A., Vincent, S.D., and Tora, L. (2022). SAGA-Dependent Histone H2Bub1 Deubiquitination Is Essential for Cellular Ubiquitin Balance during Embryonic Development. Int J Mol Sci *23*. 10.3390/ijms23137459.
59. Radmall, K.S., Shukla, P.K., Leng, A.M., and Chandrasekharan, M.B. (2023). Structure-function analysis of histone H2B and PCNA ubiquitination dynamics using deubiquitinase-deficient strains. Sci Rep *13*, 16731. 10.1038/s41598-023-43969-z.
60. Sen, R., Lahudkar, S., Durairaj, G., and Bhaumik, S.R. (2013). Functional analysis of Bre1p, an E3 ligase for histone H2B ubiquitylation, in regulation of RNA polymerase II association with active genes and transcription in vivo. J Biol Chem *288*, 9619-9633. 10.1074/jbc.M113.450403.
61. Polyansky, A.A., Gallego, L.D., Efremov, R.G., Köhler, A., and Zagrovic, B. (2023). Protein compactness and interaction valency define the architecture of a biomolecular condensate across scales. eLife *12*, e80038. 10.7554/eLife.80038.
62. Bähler, J., Wu, J.Q., Longtine, M.S., Shah, N.G., McKenzie, A., 3rd, Steever, A.B., Wach, A., Philippsen, P., and Pringle, J.R. (1998). Heterologous modules for efficient and versatile PCR-based gene targeting in Schizosaccharomyces

pombe. Yeast *14*, 943-951. 10.1002/(sici)1097-0061(199807)14:10<943::Aid-yea292>3.0.Co;2-y.
63. Lemay, J.-F., Marguerat, S., Larochelle, M., Liu, X., van Nues, R., Hunyadkürti, J., Hoque, M., Tian, B., Granneman, S., and Bähler, J. (2016). The Nrd1-like protein Seb1 coordinates cotranscriptional 3′ end processing and polyadenylation site selection. Genes & development *30*, 1558-1572.

Figure 1

A.

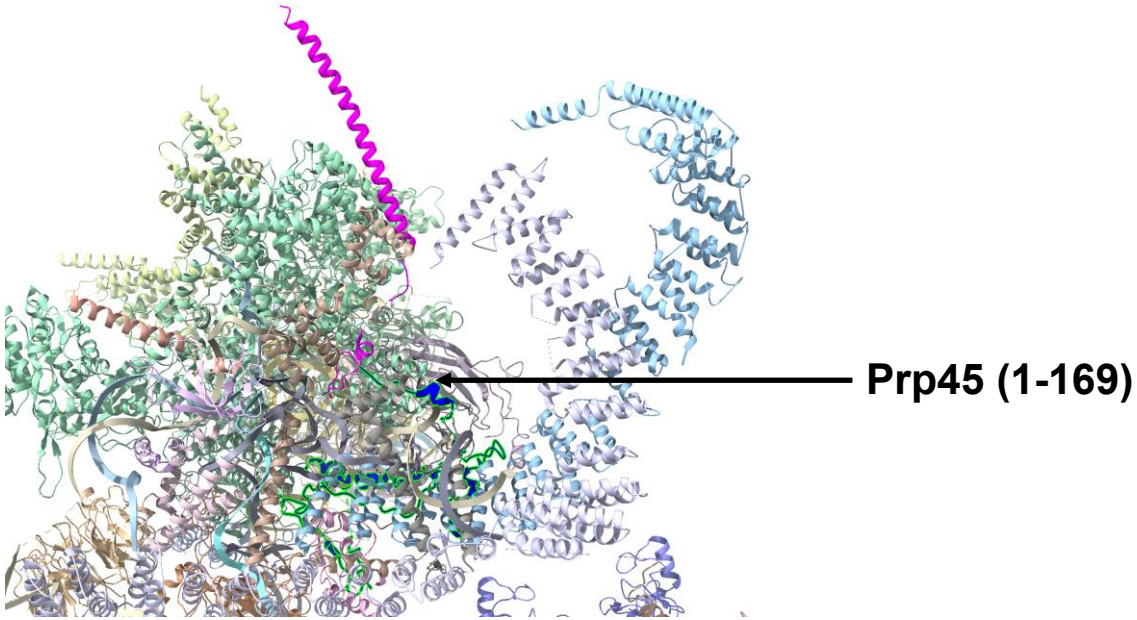
Prp45 (1-169)

B.

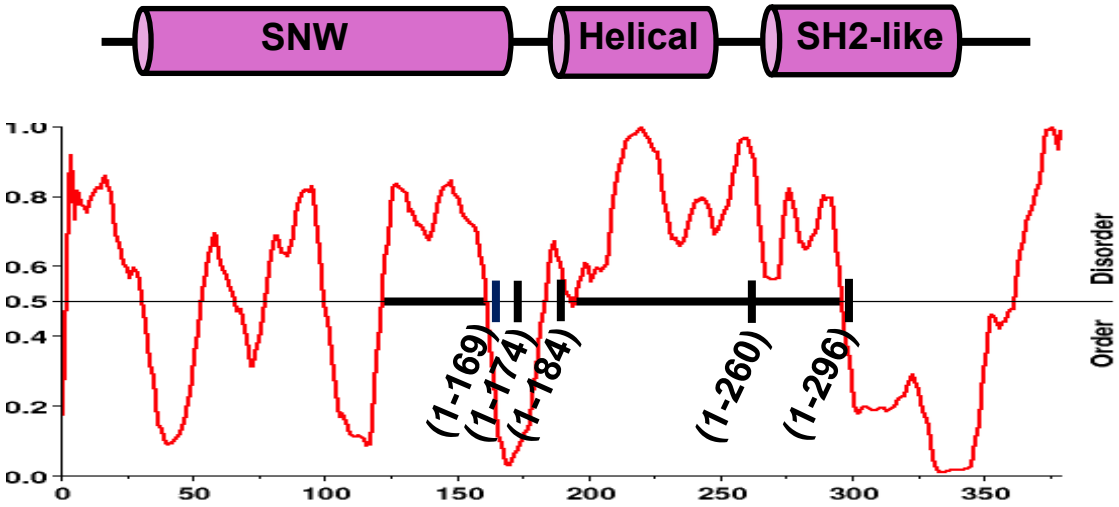
SNW
Helical
SH2-like
1.0
0.8
0.6
0.5
0.4
0.2
0.0
0
50
100
150
200
250
300
350
(1-169)
(1-174)
(1-184)
(1-260)
(1-296)
Disorder
Order

C.

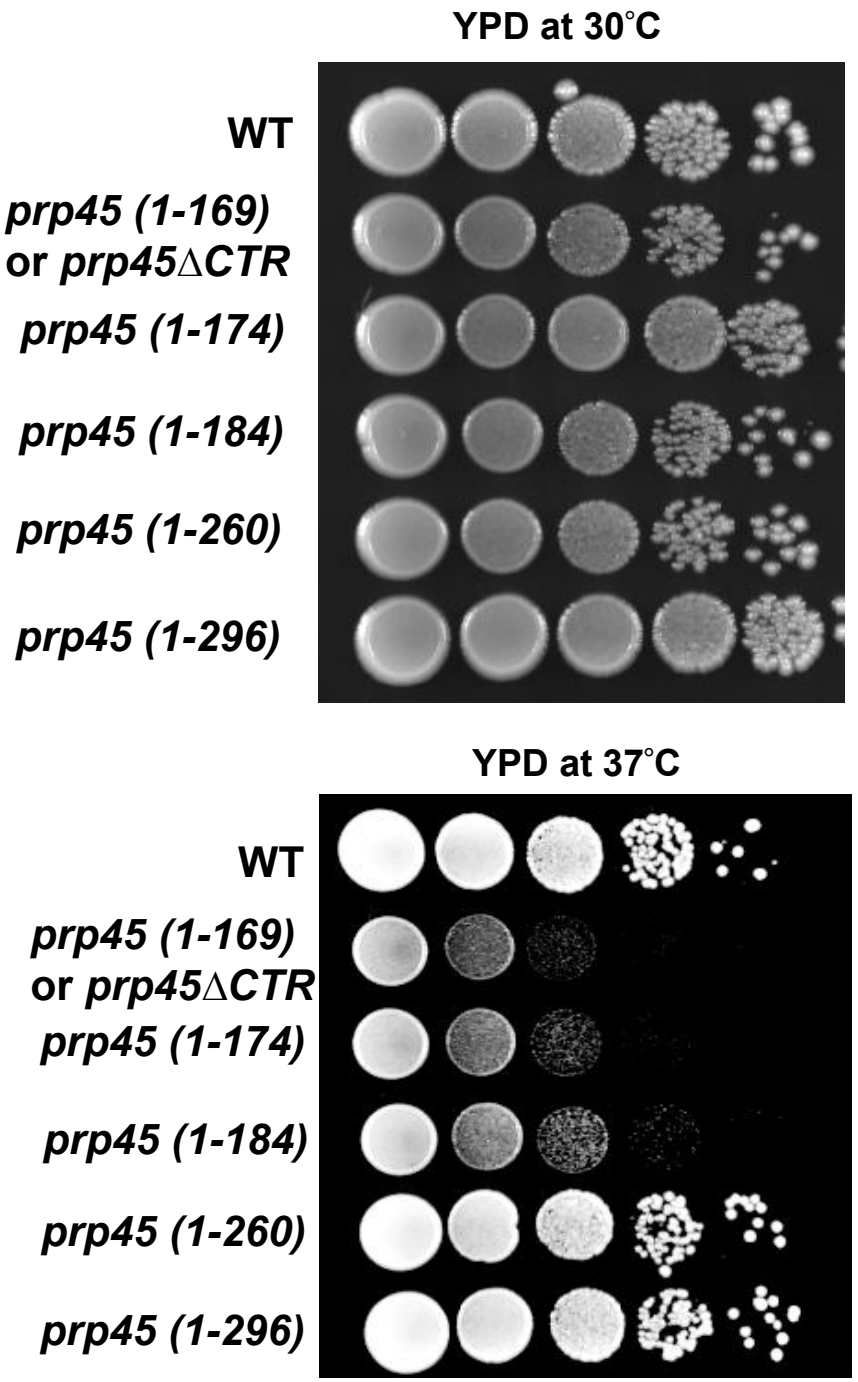
YPD at 30˚C
WT
prp45 (1-169)
or prp45ΔCTR
prp45 (1-174)
prp45 (1-184)
prp45 (1-260)
prp45 (1-296)
YPD at 37˚C
WT
prp45 (1-169)
or prp45ΔCTR
prp45 (1-174)
prp45 (1-184)
prp45 (1-260)
prp45 (1-296)

Figure 2

A.

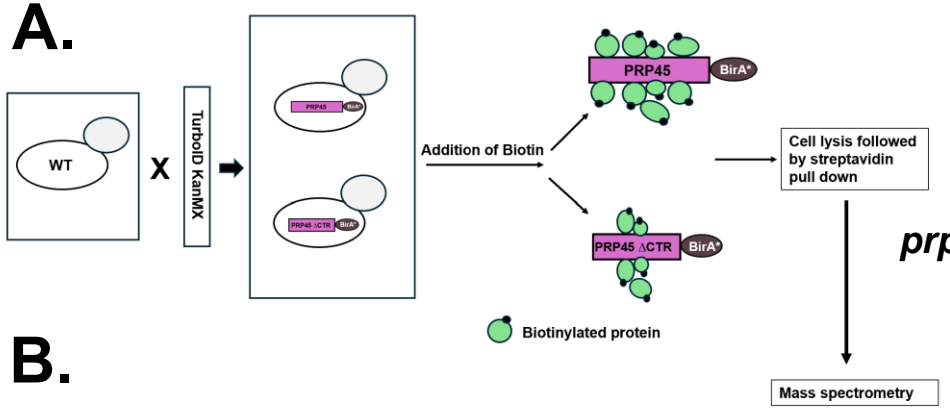
WT
X
TurboID KanMX
Addition of Biotin
PRP45
BirA*
PRP45 ΔCTR
BirA*
Biotinylated protein
Cell lysis followed by streptavidin pull down
Mass spectrometry

B.

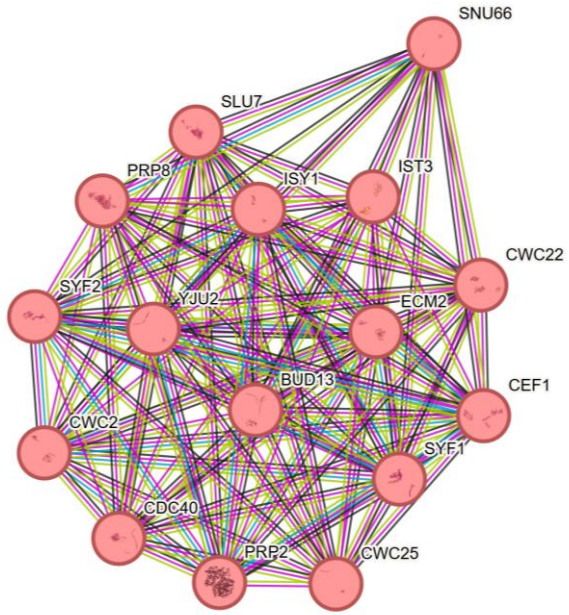
SNU66
SLU7
PRP8
ISY1
IST3
CWC22
SYF2
YJU2
ECM2
BUD13
CEF1
CWC2
SYF1
CDC40
PRP2
CWC25

C.

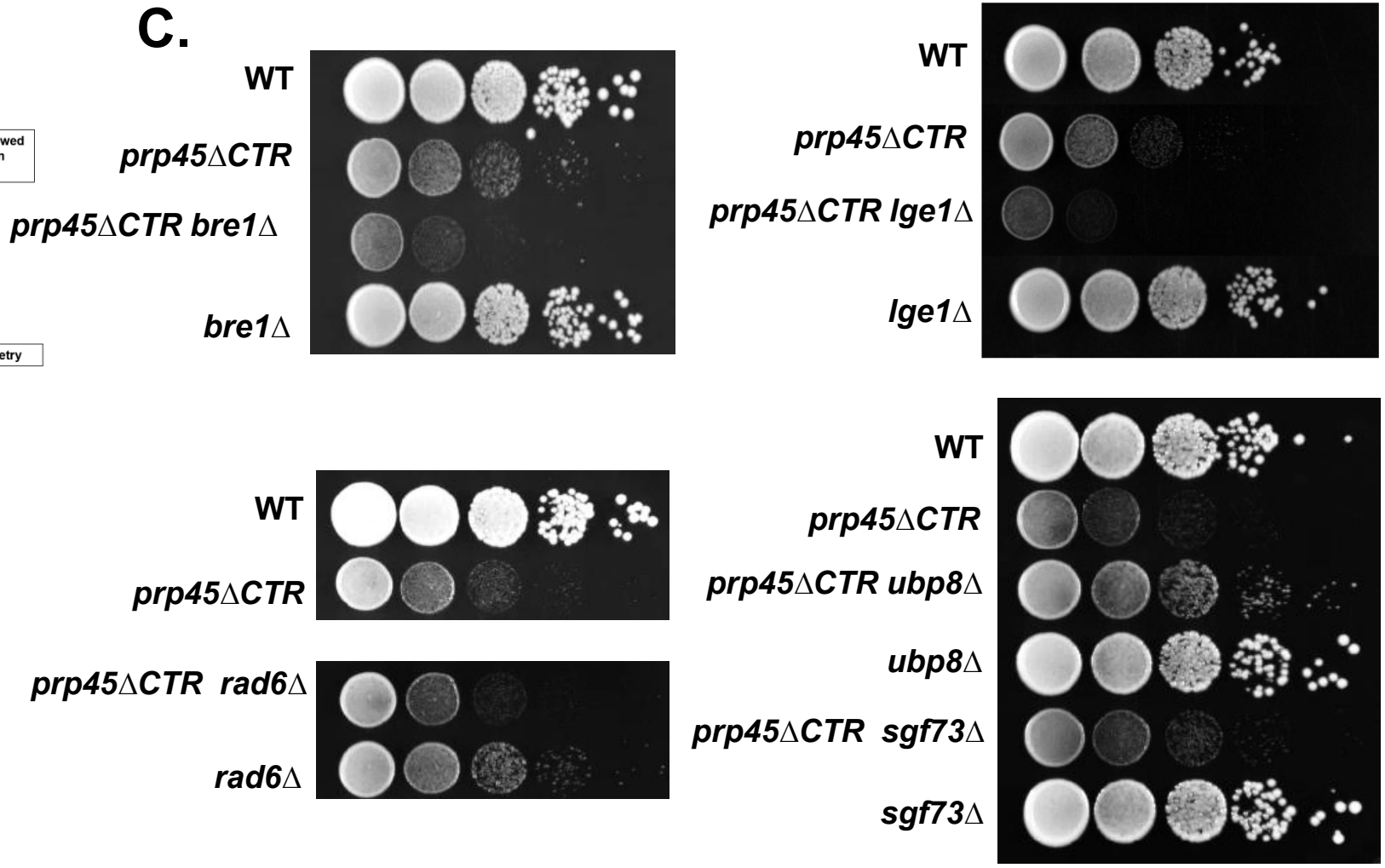
WT
prp45ΔCTR
prp45ΔCTR bre1Δ
bre1Δ
WT
prp45ΔCTR
prp45ΔCTR lge1Δ
lge1Δ
WT
prp45ΔCTR
prp45ΔCTR rad6Δ
rad6Δ
WT
prp45ΔCTR
prp45ΔCTR ubp8Δ
ubp8Δ
prp45ΔCTR sgf73Δ
sgf73Δ

Figure 3

A.

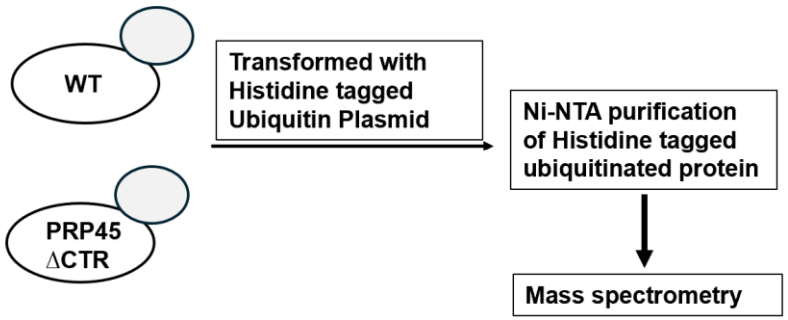

B.

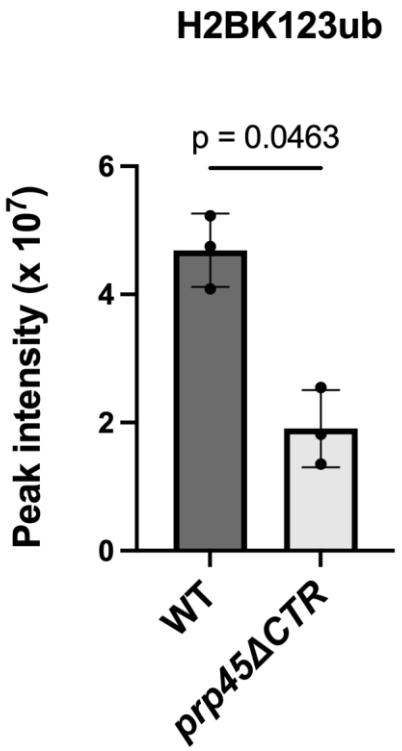

C.

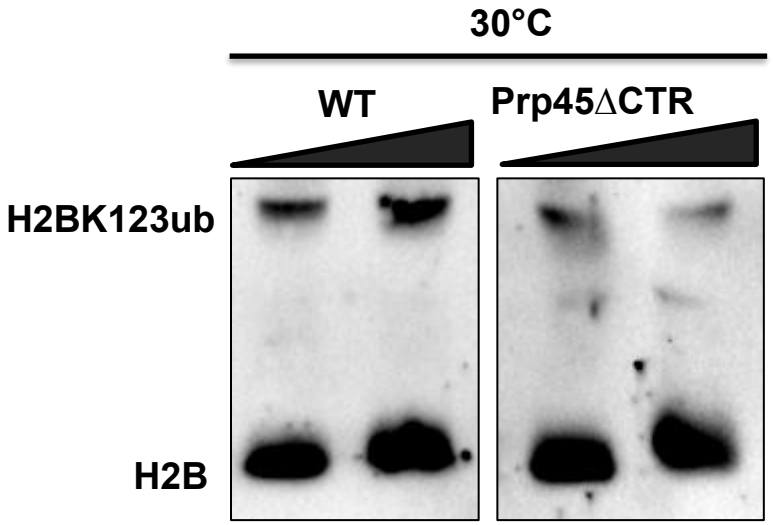

D.

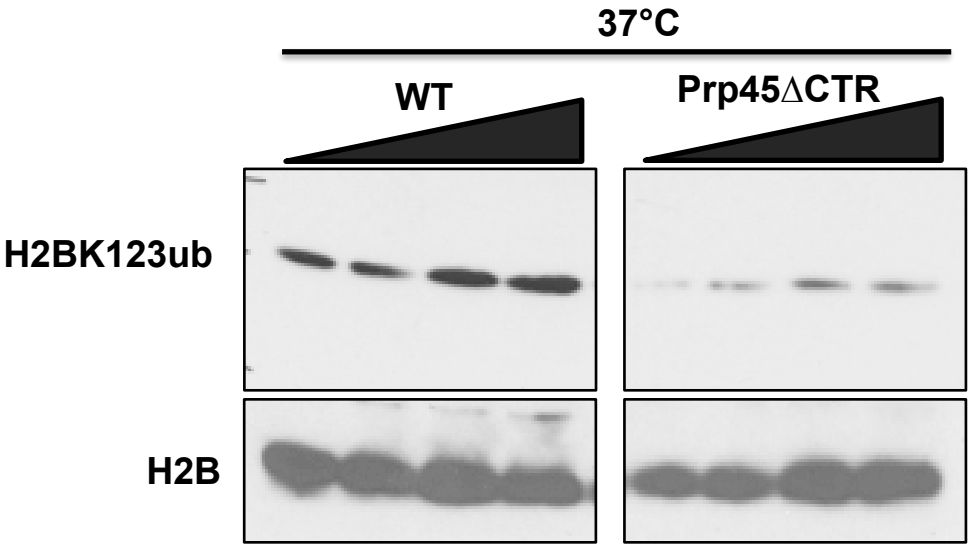

Figure 4

A.

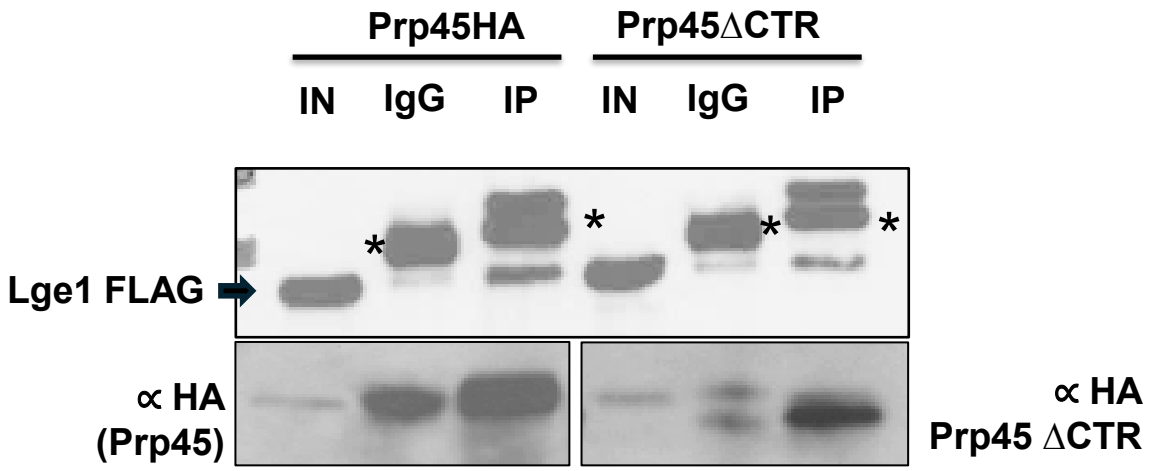

B.

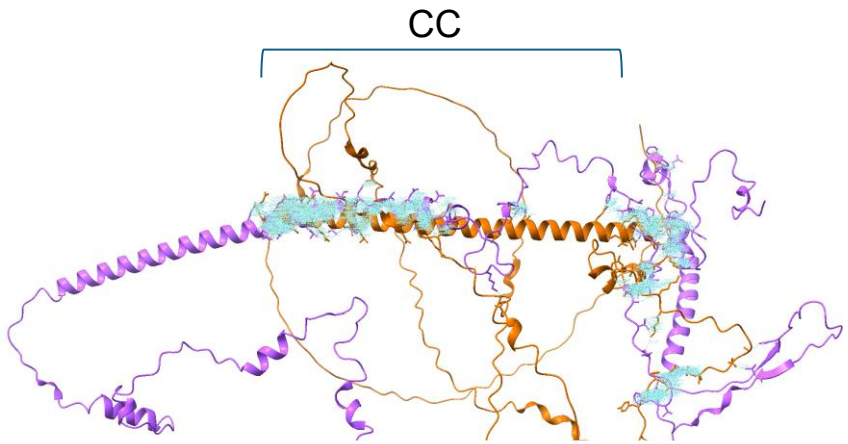

C.

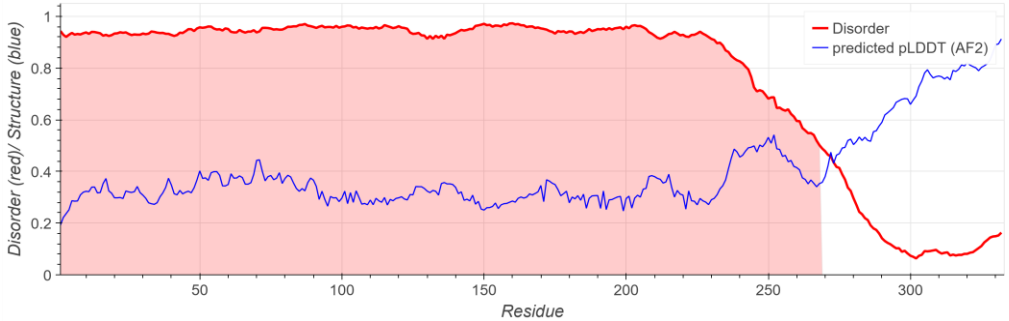

D.

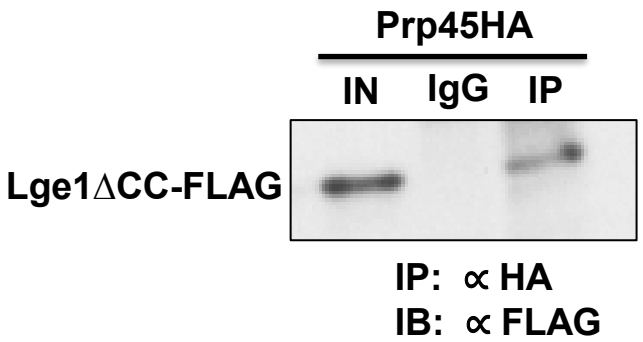

E.

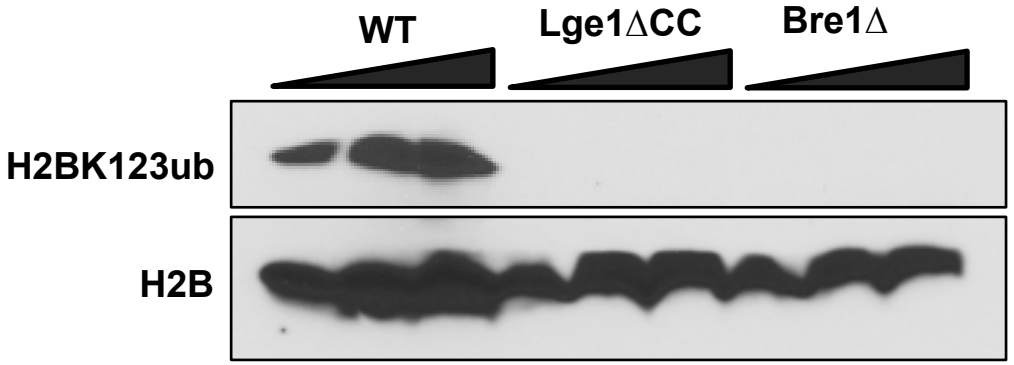

F.

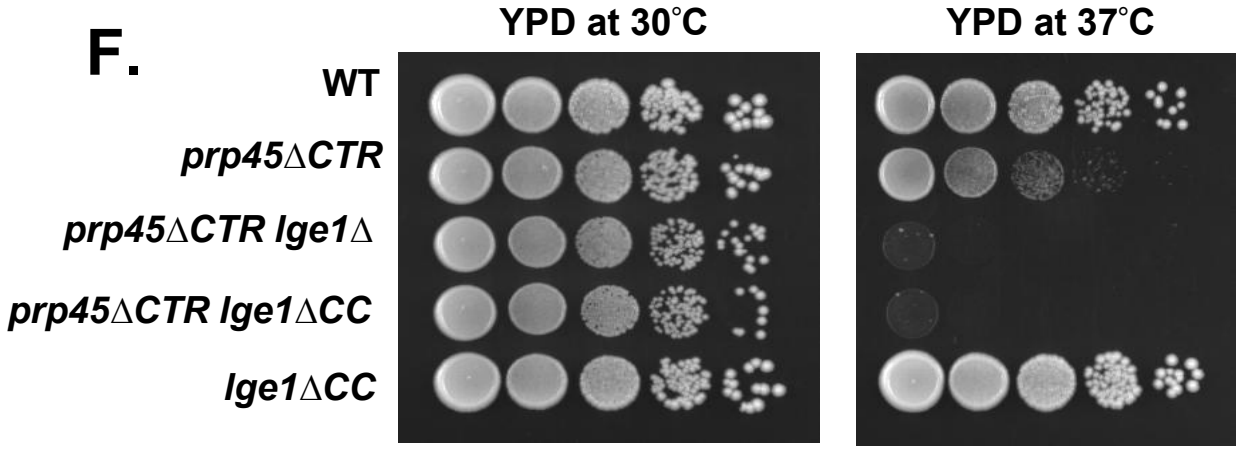

Figure 5

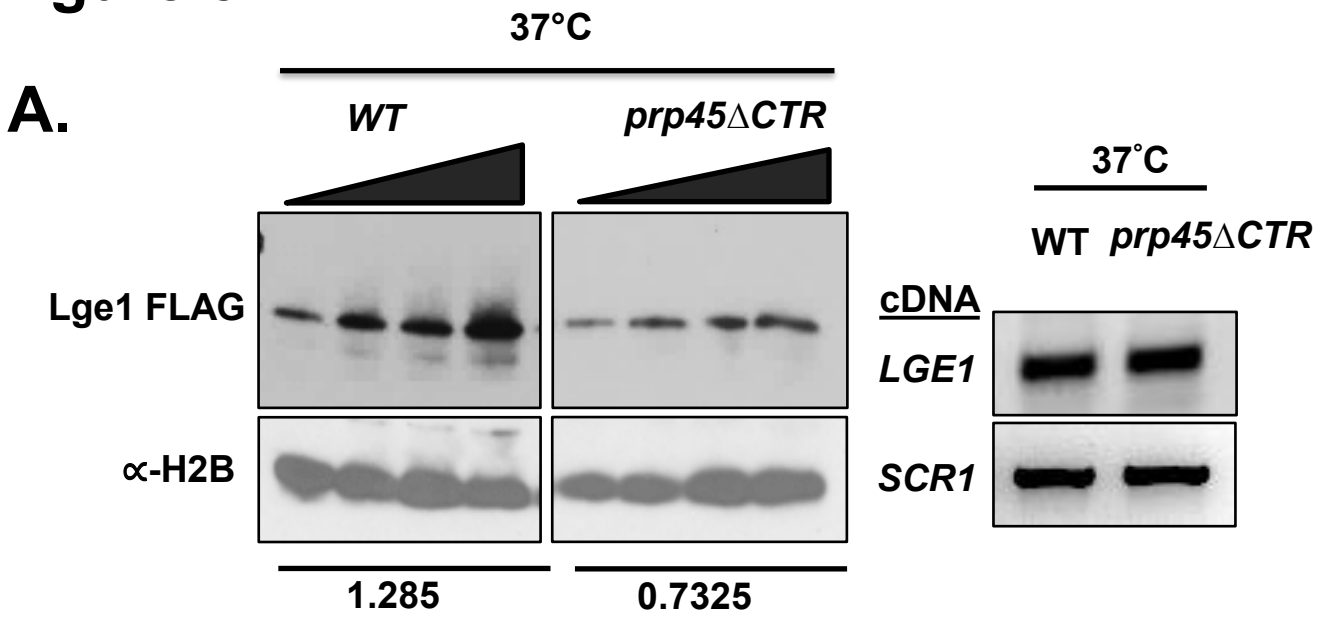
A.
37°C
WT
prp45ΔCTR
Lge1 FLAG
∝-H2B
1.285
0.7325
37˚C
WT
prp45ΔCTR
cDNA
LGE1
SCR1

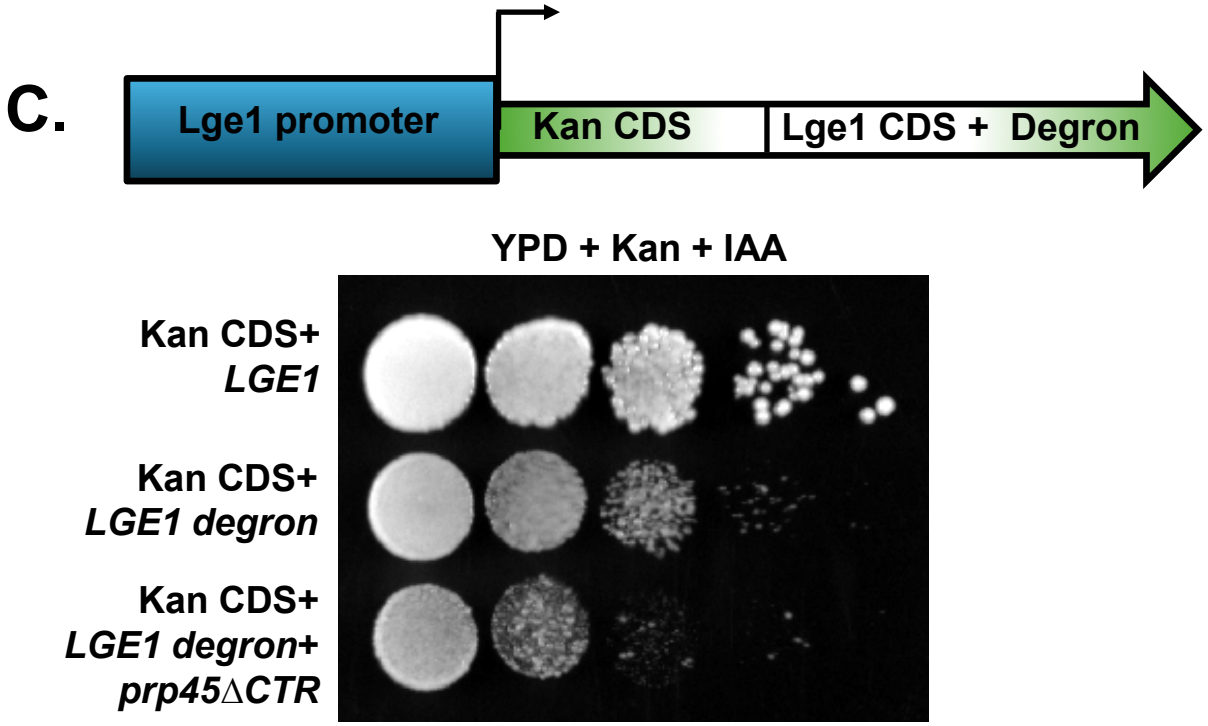
C.
Lge1 promoter
Kan CDS
Lge1 CDS + Degron
YPD + Kan + IAA
Kan CDS+
LGE1
Kan CDS+
LGE1 degron
Kan CDS+
LGE1 degron+
prp45ΔCTR

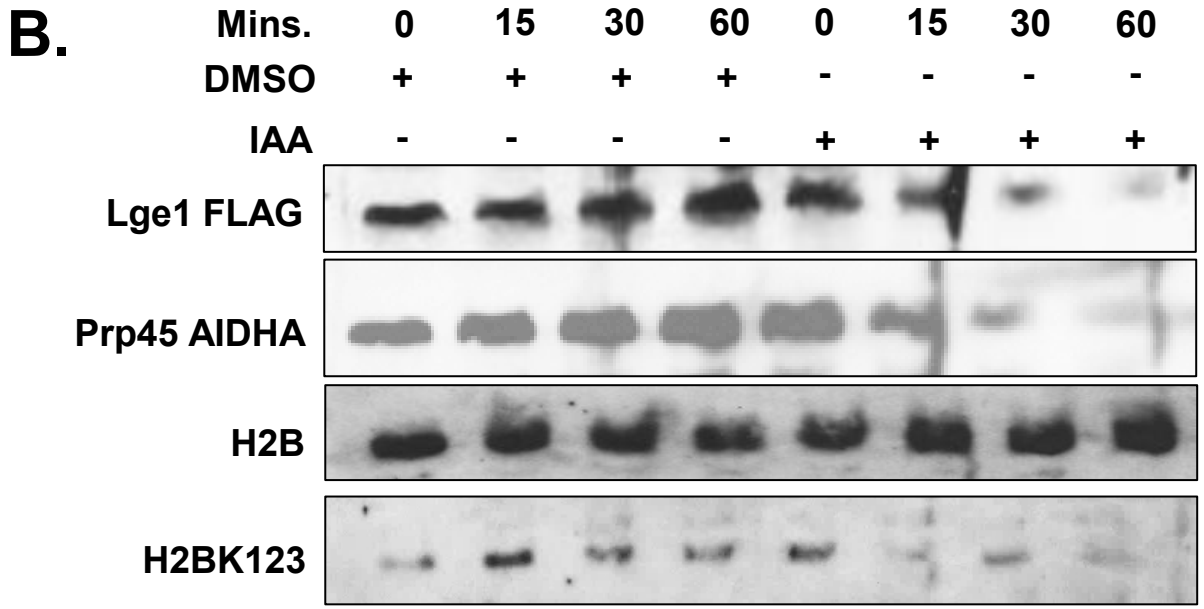
B.
Mins. 0 15 30 60 0 15 30 60
DMSO + + + + - - - -
IAA - - - - + + + +
Lge1 FLAG
Prp45 AIDHA
H2B
H2BK123

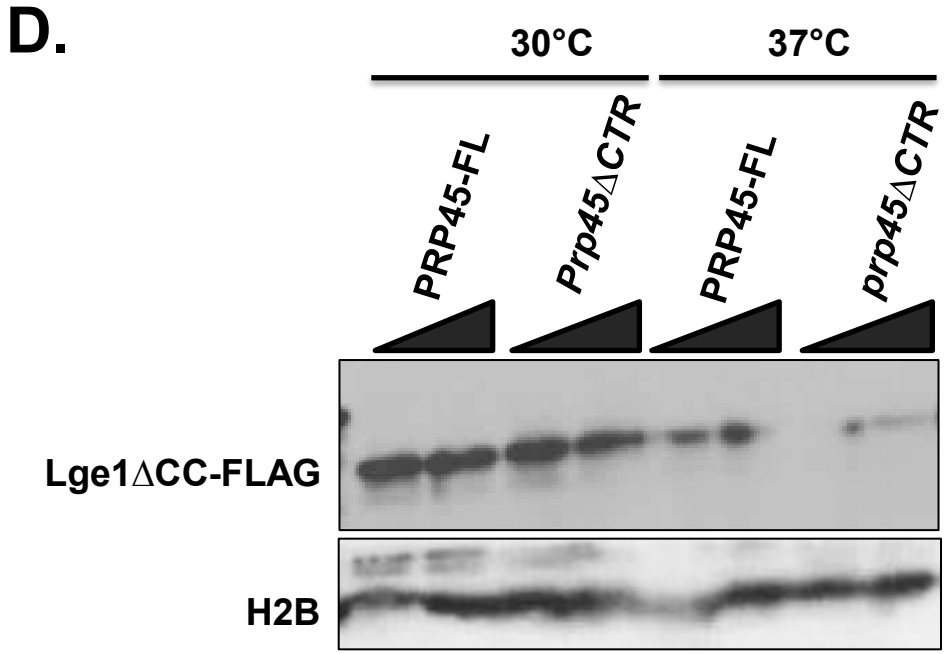
D.
30°C
37°C
PRP45-FL
Prp45ΔCTR
PRP45-FL
prp45ΔCTR
Lge1ΔCC-FLAG
H2B

Figure 6

A.

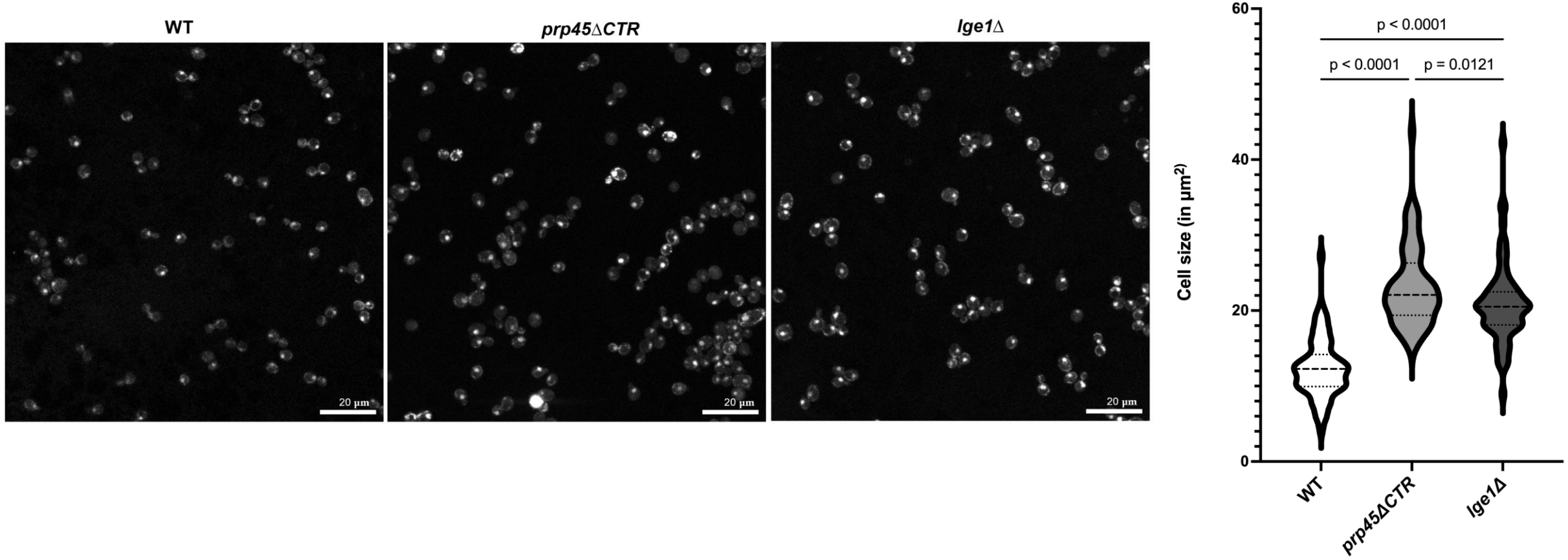
WT
prp45ΔCTR
lge1Δ
20 µm
20 µm
20 µm
Cell size (in µm²)
60
40
20
0
p < 0.0001
p < 0.0001
p = 0.0121
WT
prp45ΔCTR
lge1Δ

Figure 6

B.

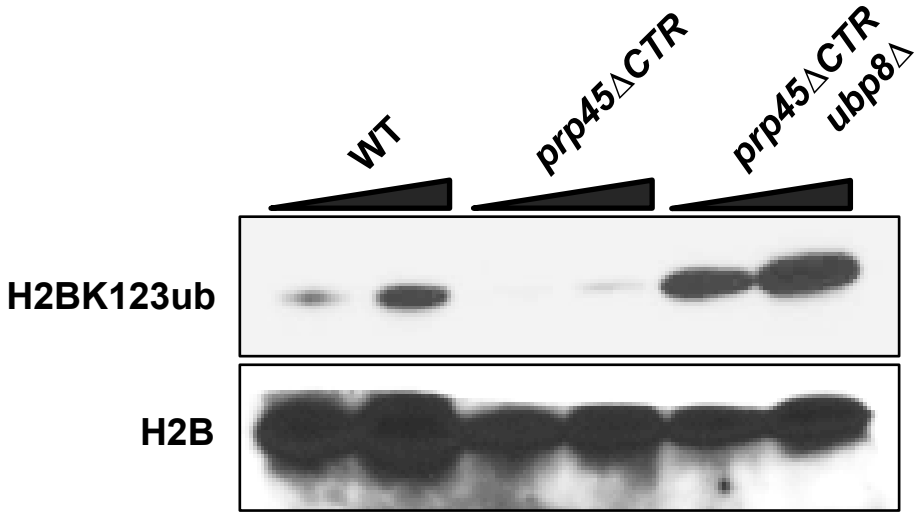
WT
prp45ΔCTR
prp45ΔCTR ubp8Δ
H2BK123ub
H2B

C.

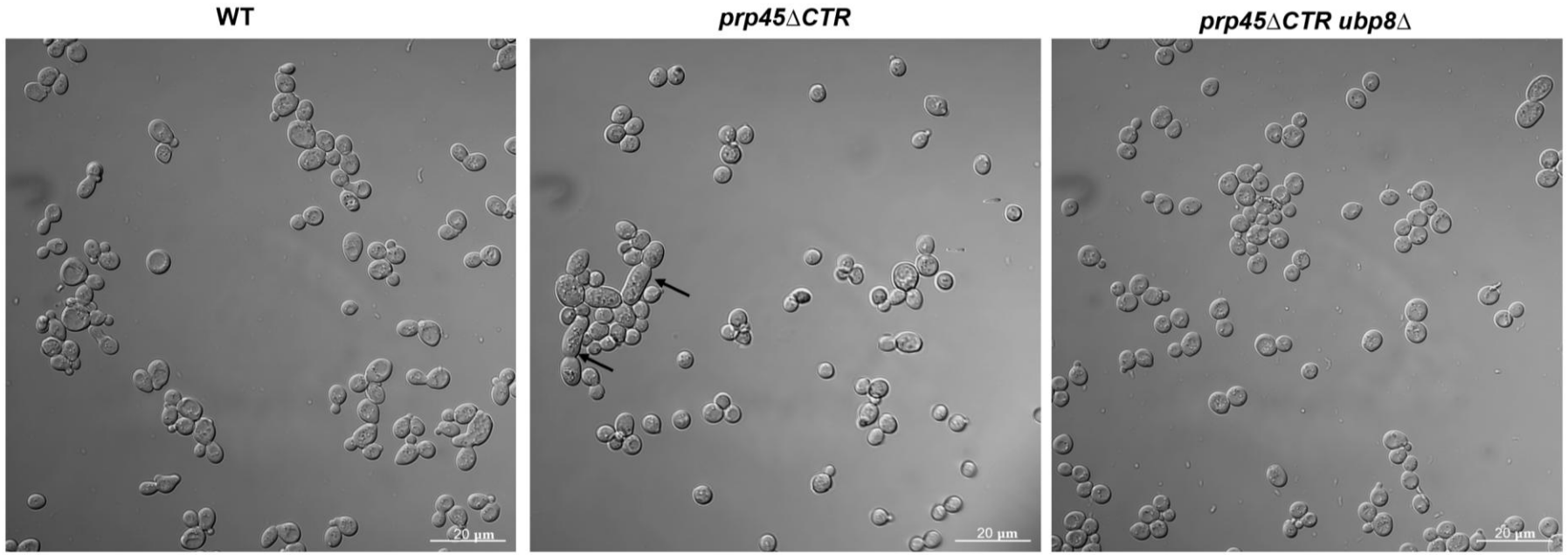
WT
prp45ΔCTR
prp45ΔCTR ubp8Δ
20 µm
20 µm
20 µm

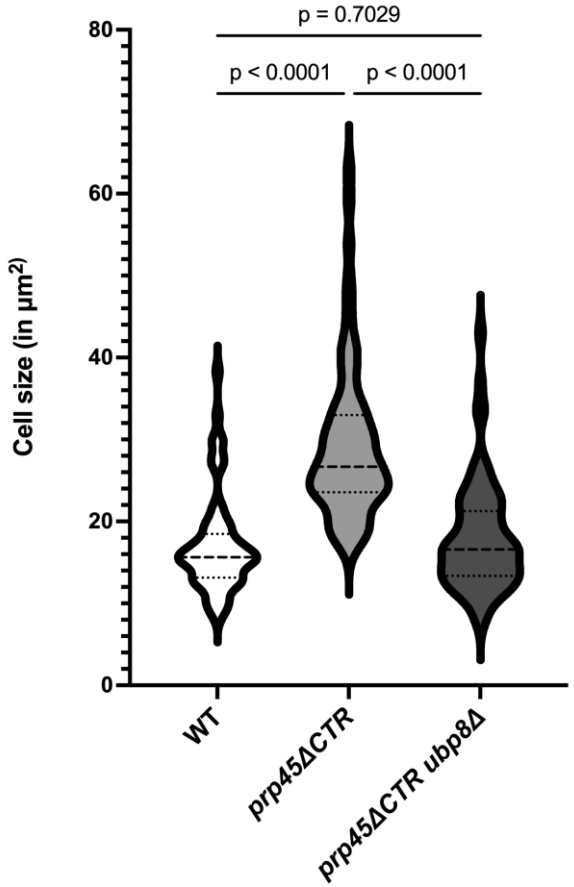
p = 0.7029
p < 0.0001
p < 0.0001
Cell size (in µm²)
0
20
40
60
80
WT
prp45ΔCTR
prp45ΔCTR ubp8Δ

Figure 6

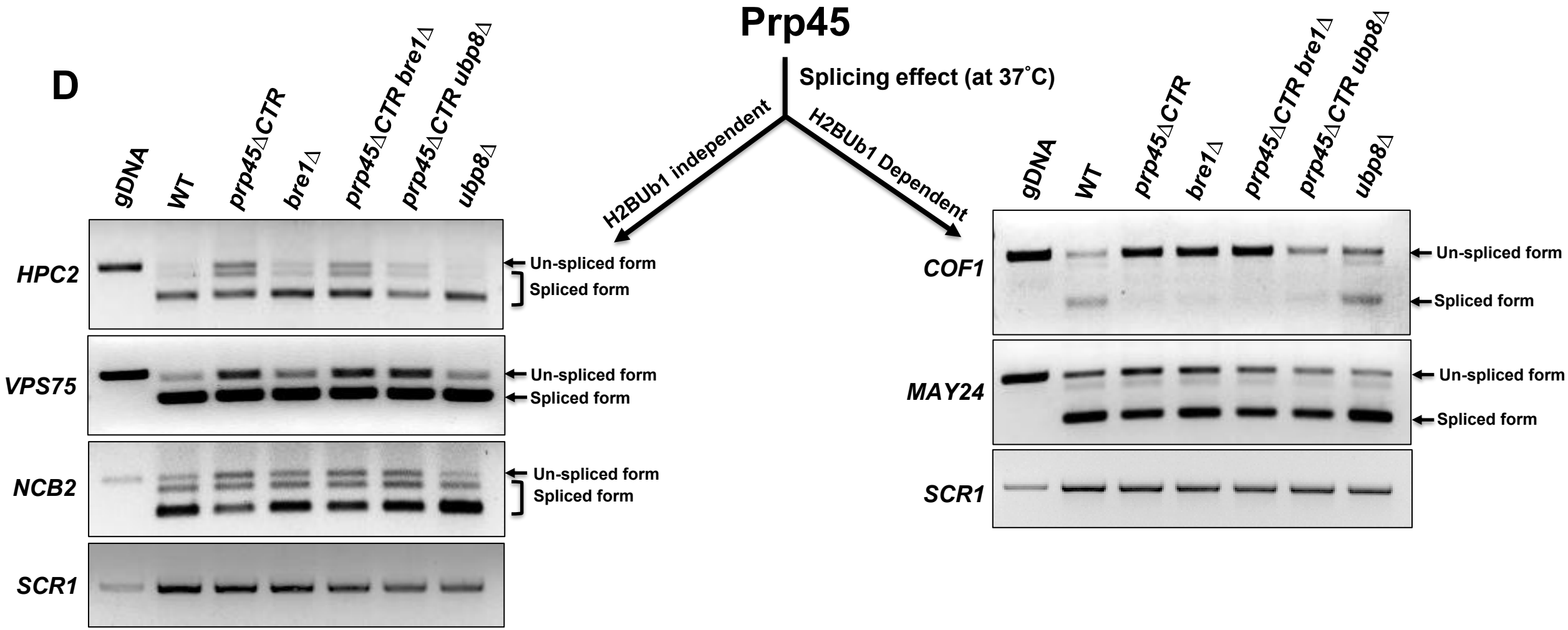
D
Prp45
Splicing effect (at 37˚C)
H2BUb1 independent
H2BUb1 Dependent
gDNA
WT
prp45ΔCTR
bre1Δ
prp45ΔCTR bre1Δ
prp45ΔCTR ubp8Δ
ubp8Δ
HPC2
VPS75
NCB2
SCR1
Un-spliced form
Spliced form
COF1
MAY24

Figure 7 Model

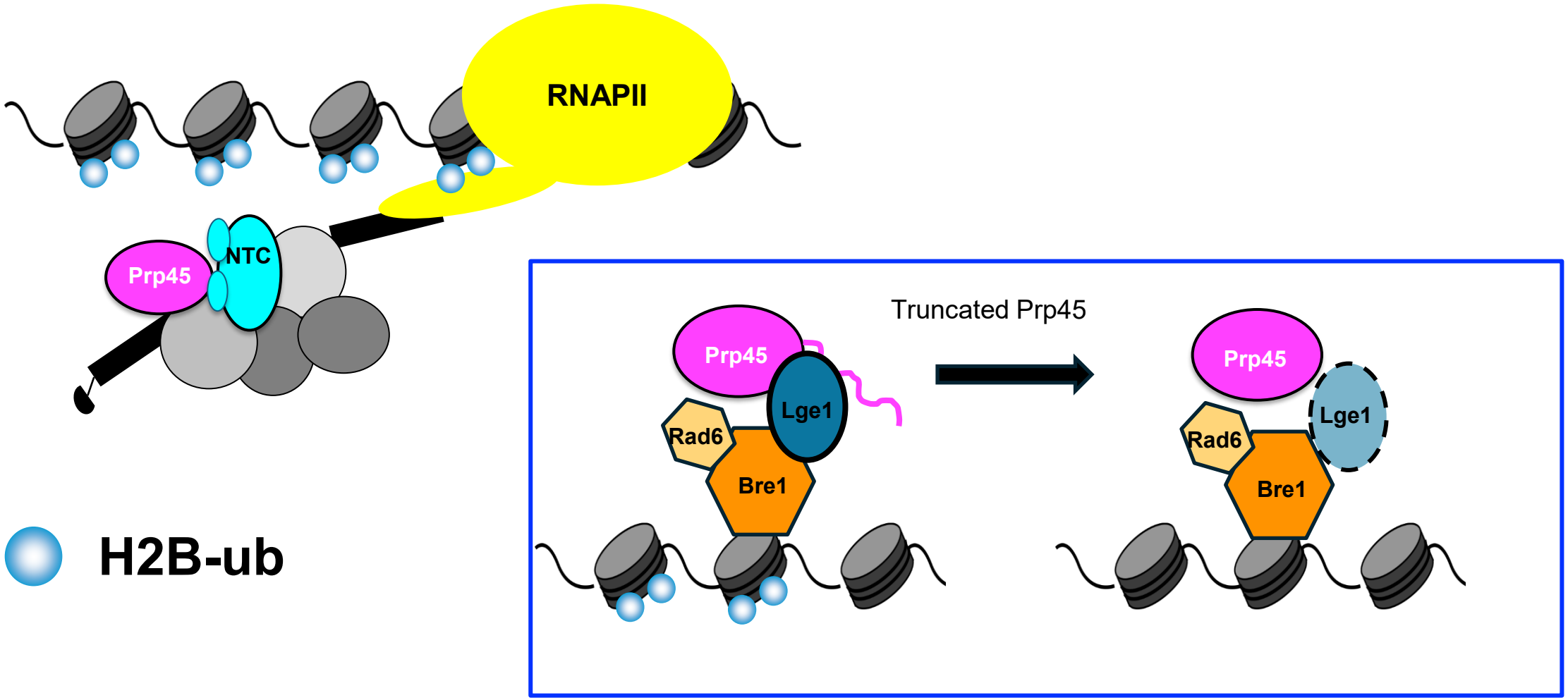

Supplement 1 (Related to figure 2)

A.

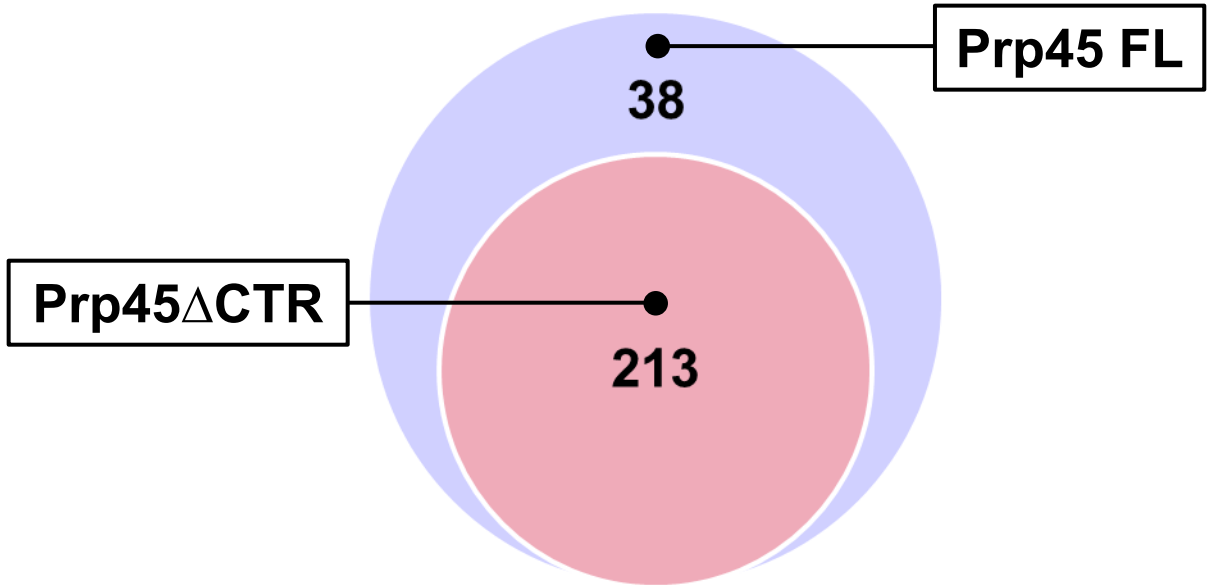

B.

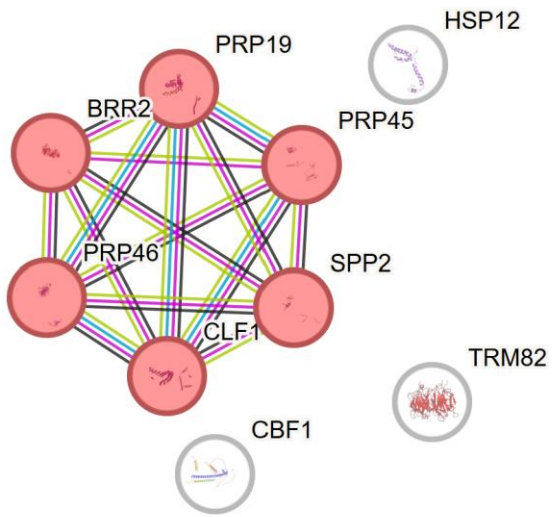

Table (Related to figure 2)

Serial no.	Proteins lost interaction with Prp45ΔCTR
1	CWC25
2	BUD13
3	SYF2
4	CDC40
5	PRP8
6	CTK1
7	PRP2
8	CEF1
9	SLU7
10	IST3
11	SGV1
12	HSF1
13	ISY1
14	RIX1
15	MRC1
16	KRI1
17	ECM16
18	ECM2
19	GCD10
20	CWC22
21	HRP1
22	RNR4
23	LRP1
24	REB1
25	UBA2
26	IMP4
27	SNU66
28	FDO1
29	BRE1
30	RFC5
31	GRX1
32	SIR4
33	TOD6
34	IGD1
35	MBF1
36	NUP1
37	SIR2
38	SYF1

Supplement 2 (Related to figure 2)

A.

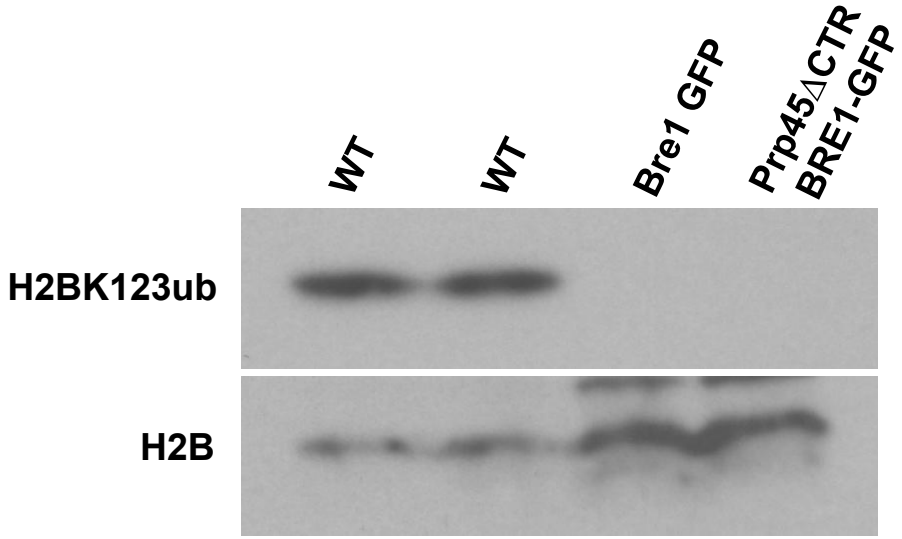

B.

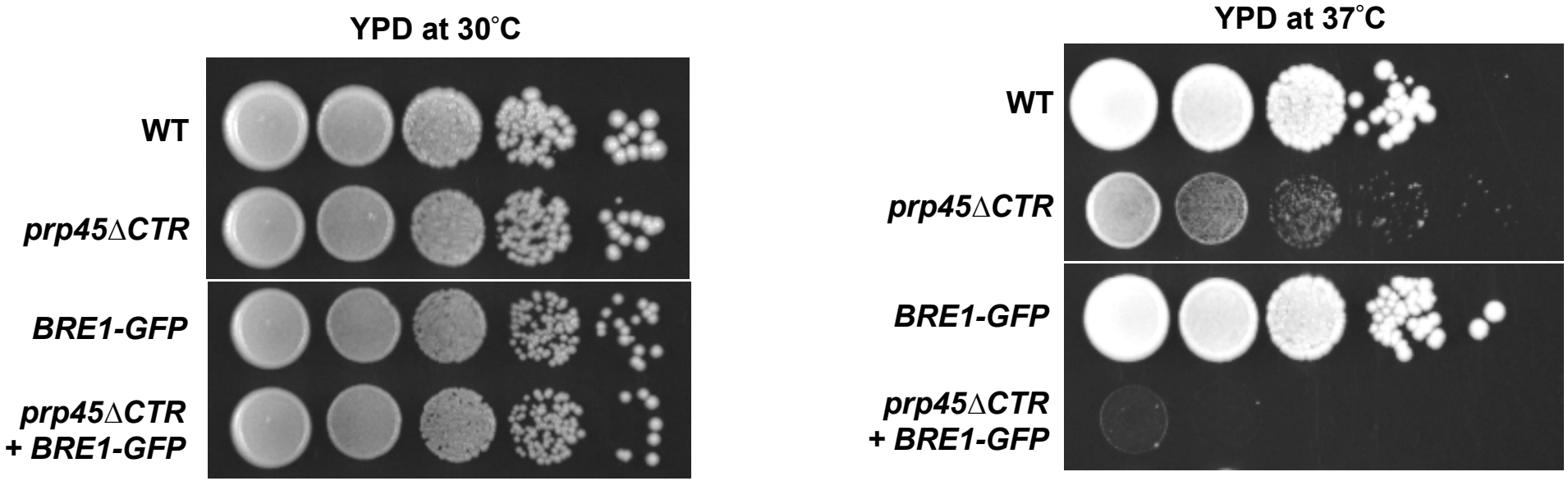

Supplement 3 (Related to figure 2)

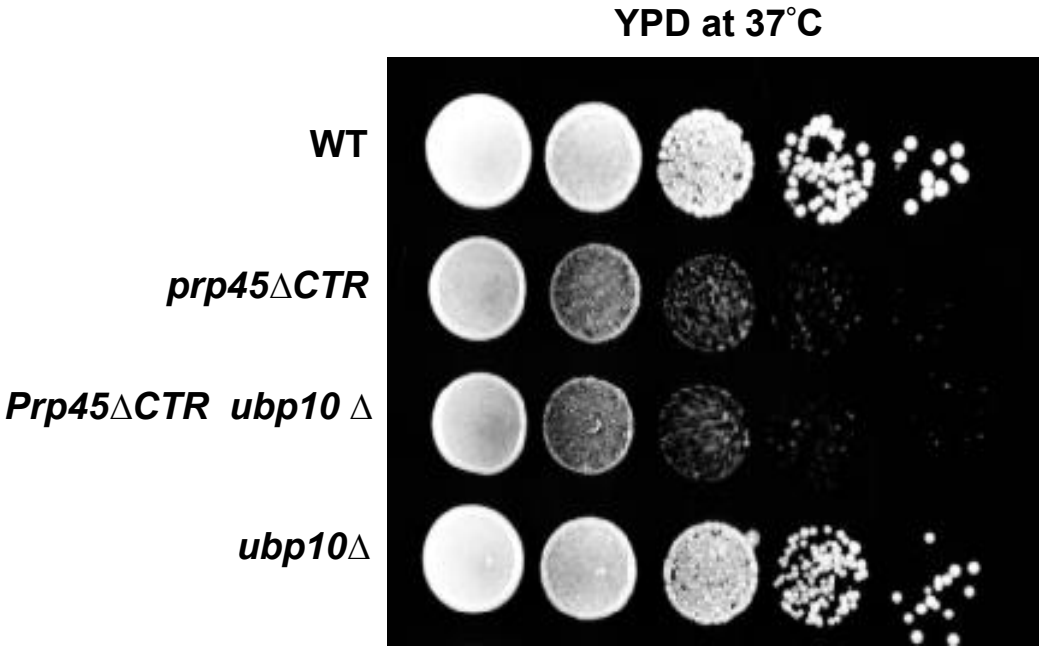
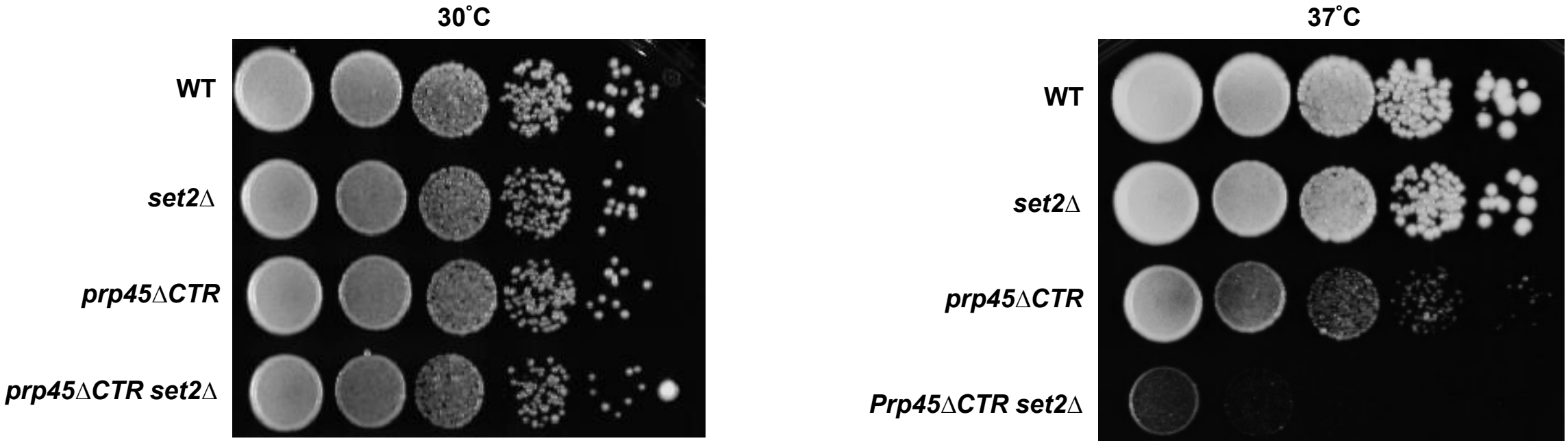
Supplement 4